NAVAL POSTGRADUATE SCHOOL
Monterey, California

THESIS

CIRCUIT MODELS FOR A MILLIMETER-WAVE SUSPENDED-MICROSTRIP LINE DISCONTINUITY

by

Won Tae Jin

September, 1990

Thesis Advisor: Harry A. Atwater

UCLASSIFIED
SECURITY CLASSIFICATION OF THIS PAGE

REPORT DOCUMENTATION PAGE

Form Approved
OMB No 0704-0188

1a REPORT SECURITY CLASSIFICATION: Uclassified	1b RESTRICTIVE MARKINGS
2a SECURITY CLASSIFICATION AUTHORITY	3 DISTRIBUTION/AVAILABILITY OF REPORT: Approved for public release; distribution is unlimited.
2b DECLASSIFICATION/DOWNGRADING SCHEDULE	
4 PERFORMING ORGANIZATION REPORT NUMBER(S)	5 MONITORING ORGANIZATION REPORT NUMBER(S)
6a NAME OF PERFORMING ORGANIZATION: Naval Postgraduate School; 6b OFFICE SYMBOL (If applicable): 3A	7a. NAME OF MONITORING ORGANIZATION: Naval Postgraduate School
6c. ADDRESS (City, State, and ZIP Code): Monterey, CA 93943-5000	7b ADDRESS (City, State, and ZIP Code): Monterey, CA 93943-5000
8a NAME OF FUNDING/SPONSORING ORGANIZATION; 8b OFFICE SYMBOL (If applicable)	9 PROCUREMENT INSTRUMENT IDENTIFICATION NUMBER
8c. ADDRESS (City, State, and ZIP Code)	10 SOURCE OF FUNDING NUMBERS: PROGRAM ELEMENT NO; PROJECT NO; TASK NO; WORK UNIT ACCESSION NO

11 TITLE (Include Security Classification): CIRCUIT MODELS FOR A MILLIMETER-WAVE SUSPENDED-MICROSTRIP LINE DISCONTINUITY

12 PERSONAL AUTHOR(S): Won Tae Jin

13a TYPE OF REPORT	13b TIME COVERED	14 DATE OF REPORT (Year, Month, Day)	15 PAGE COUNT
Master's Thesis	FROM _____ TO _____	September 1990	74

16 SUPPLEMENTARY NOTATION: The views expressed in this thesis are those of the author and do not reflect the official policy or position of the U. S. Government

17 COSATI CODES			18 SUBJECT TERMS (Continue on reverse if necessary and identify by block number)
FIELD	GROUP	SUB-GROUP	Suspended-microstrip line, Step discontinuity Equivalent circuit model, step-change

19 ABSTRACT (Continue on reverse if necessary and identify by block number)

The goal of this work is to develop an equivalent circuit model for a typical discontinuity in shielded suspended substrate line, in particular, the step-change in width. This circuit model is needed for use in CAD analysis of microwave systems using the suspended stripline transmission mode.

20 DISTRIBUTION/AVAILABILITY OF ABSTRACT	21 ABSTRACT SECURITY CLASSIFICATION
☒ UNCLASSIFIED/UNLIMITED ☐ SAME AS RPT ☐ DTIC USERS	Unclassified
22a NAME OF RESPONSIBLE INDIVIDUAL: Harry A. Atwater	22b TELEPHONE (Include Area Code): (408) 646-3001; 22c OFFICE SYMBOL: 62An

DD Form 1473, JUN 86 — Previous editions are obsolete — S/N 0102-LF-014-6603

SECURITY CLASSIFICATION OF THIS PAGE
Unclassified

Approved for public release; distribution is unlimited.

Circuit Models for a Millimeter-wave
Suspended-microstrip Line Discontinuity

by

Won Tae Jin
Major, Republic of Korea Army
B.S., Korea Military Academy, 1981

Submitted in partial fulfillment
of the requirements for the degree of

MASTER OF SCIENCE IN SYSTEMS ENGINEERING
(ELECTRONIC WARFARE)

from the

NAVAL POSTGRADUATE SCHOOL
September 1990

Author: Won Tae Jin

Won Tae Jin

Approved by: H. A. Atwater

Harry A. Atwater, Thesis Advisor

R Janaswamy

Rama Janaswamy, Second Reader

Joseph Sternberg

Joseph Sternberg, Chairman
Electronic Warfare Academic Group

ABSTRACT

The goal of this work is to develop an equivalent circuit model for a typical discontinuity in shielded suspended substrate line, in particular, the step-change in width. This circuit model is needed for use in CAD analysis of microwave systems using the suspended stripline transmission mode.

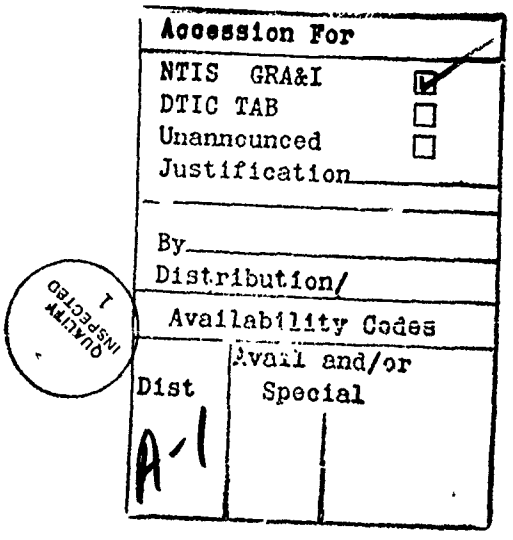

TABLE OF CONTENTS

LIST OF TABLES

LIST OF FIGURES

I. INTRODUCTION

The shielded suspended substrate line (SSSL) is a transmission medium useful for radar and circuits at microwave and millimeter-wave frequencies. In order to use this transmission medium in the construction of microwave circuits and filters, it is necessary to have valid circuit models for typical discontinuities such as the series gap in line, open-ended stub, and a discontinuous change in width.

There is a definite need for an accurate full-wave analysis of strip transmission line structures. Even though many studies have been performed for the discontinuities of conventional microstrip line, almost no discontinuity calculations are available for SSSL. By full-wave analysis is implied the process of rigorously solving the frequency-dependent electromagnetic (EM) boundary value problem with retention of all the field components.

In this thesis, the discontinuity structure of interest incorporated in a SSSL resonator has been calculated by a formulation employing full-wave analysis. The solution of the problem has been derived using an efficient method. Specifically, the derivation of the characteristic equation for resonant frequencies of the resonator model is carried out using Galerkin's technique applied in the spectral or Fourier transform domain instead of the space domain. The resonant frequencies of the structures of interest are obtained by numerically solving the characteristic

equation. The details of the analysis method will appear in Section II of this work.

In Section III, the step discontinuity will be analyzed by placing the discontinuity in an open-ended strip line resonator. In the continuous strip case, the strip line has no discontinuity step in width. Following this, the equivalent circuit of the discontinuity will be deduced from the numerical resonance data for the embedding SSSL resonator when the discontinuity is inserted.

II. THEORETICAL ANALYSIS

The microstrip resonator to be analyzed is shown in Fig.1. A strip transmission line which has a step in width is placed on the suspended substrate. The shielded suspended substrate line is constructed by placing the substrate within a channel milled in the sidewalls. Selection of both depth and width of the shield enclosure is important. Dimensions must be sufficiently small to avoid propagation of waveguide modes within the shield: these modes would actually produce an unwanted coupling with the resonance one is trying to detect. On the other hand, if the enclosure dimensions are too small, the propagation characteristics of the transmission line itself would be significantly modified.

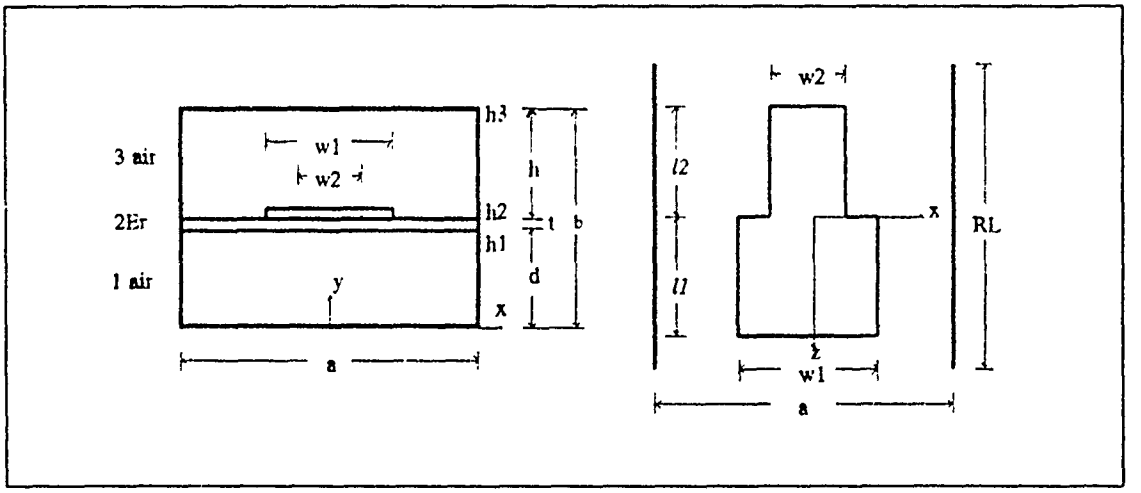

Figure 1 End and top view of suspended substrate microstrip line

It is assumed that the thickness of the conducting strip is negligible and that all the media and conductors are lossless. For simplicity, the strip is assumed to be located symmetrically in the longitudinal direction within the ends of the shielding enclosure.

A. FOURIER-TRANSFORMED GALERKIN'S METHOD FOR THE SHIELDED STRIP RESONATOR

The analysis of wave propagation on shielded strip transmission systems of the type considered here has been carried out by Itoh and Uwano [Ref.2]. These authors treated the problem using Galerkin's method of moments in the Fourier-Transform domain. Their work is summarized in terms of a set of Green's function equations:

$$\tilde{Z}_{zz}\tilde{J}_z + \tilde{Z}_{zx}\tilde{J}_x = \tilde{E}_z \tag{1a}$$

$$\tilde{Z}_{xz}\tilde{J}_z + \tilde{Z}_{xx}\tilde{J}_x = \tilde{E}_x \tag{1b}$$

In Eqs. (1a) and (1b), J_z and J_x are the z and x components of the currents on the strip conductor, and E_z and E_x are the components of electric field tangent to the substrate surface, and the Z_{ij} are the Green's functions.

The tildes over the factors in Eqs.(1a) and (1b) imply Fourier transformation of the respective quantities. In this work, the Fourier transformation is carried out in the bounded region interior to the shielding enclosure placed around the line segment representing the resonator. Therefore we have the finite Fourier transformation:

$$\tilde{f}(k_n, \beta_m) = \int_{-\frac{RL}{2}}^{\frac{RL}{2}} \int_{-\frac{a}{2}}^{\frac{a}{2}} f(x, y, z)\, e^{jk_n x} e^{j\beta_m z} dx dz \qquad (2a)$$

where k_n and β_m are the discrete transform variables defined by,

$k_n = (n-1/2)\pi/a$ for E_z even, $-H_z$ odd(in x) modes (2b)

$k_n = n\pi/a$ for E_z odd, $-H_z$ even(in x) modes (2c)

$\beta_m = (m-1/2)\pi/RL$ for E_z even, $-H_z$ odd(in z) modes (2d)

$\beta_m = m\pi/RL$ for E_z odd, $-H_z$ even(in z) modes (2e)

where a is width of waveguide, and RL is length of waveguide enclosure.

The analytical task then consists of assuming suitable coordinate forms of the current densities J_z and J_x, and Fourier-transforming these. Inner products are then formed in Eqs (1a) and (1b), in accordance with the standard procedure of the method of moments. This procedure gives rise to a set of homogeneous equations in the unknown coefficients assumed in J_z and J_x. The solution condition for the simultaneous equations leads to a determination of the resonance frequency of the strip line resonator of the problem. The unknowns E_z and E_x can be eliminated by applying Galerkin's method in the spectral domain. The first step is to expand the unknowns J_z and J_x in terms of assumed basis functions J_{zm} and J_{xm} with unknown coefficients c_m and d_m .

$$\tilde{J}_z(k_n, \beta_m) = \sum_{m=1}^{N} d_m \tilde{J}_{zm}(k_n, \beta_m) \tag{3a}$$

$$\tilde{J}_x(k_n, \beta_m) = \sum_{m=1}^{M} c_m \tilde{J}_{xm}(k_n, \beta_m) \tag{3b}$$

The basis functions $\tilde{J}_{zm}$ and $\tilde{J}_{xm}$ must be chosen to be the Fourier transforms of space-domain functions $J_{zm}(x,z)$ and $J_{xm}(x,z)$ which are physically realistic, and which are zero except for the region $|x| < w_1$ and $|z| < \ell$. Substituting (3) into (1) and taking inner products of the resulting equations with the basis function and for different values of i yields the matrix equations,

$$\tilde{J}_{zi}\tilde{Z}_{zz}\sum_{m=1}^{N} c_m \tilde{J}_{zm} + \tilde{J}_{zi}\tilde{Z}_{zx}\sum_{m=1}^{M} d_m \tilde{J}_{xm} = 0 \qquad i=1,2,..,M \tag{4a}$$

$$\tilde{J}_{xi}\tilde{Z}_{xz}\sum_{m=1}^{N} c_m \tilde{J}_{zm} + \tilde{J}_{xi}\tilde{Z}_{xx}\sum_{m=1}^{M} d_m \tilde{J}_{xm} = 0 \qquad i=1,2,..,N \tag{4b}$$

The right-hand sides of (4) are zero by virtue of Parseval's theorem, because the currents $J_{zi}(x)$, $J_{xi}(x)$ and the field components $E_z(x,h_2)$, $E_x(x,h_2)$ vanish in

complementary regions of x. For example, if the inner product of $\tilde{E}_z$ on the right-hand side of Eq.(1) with $\tilde{J}_{zi}(k_n)$ is taken, one obtains:

$$\int_{-\infty}^{\infty} \tilde{J}_{zi}(k_n)\,\tilde{E}_z(k_n)\,dk_n = 2\pi \int_{-\frac{a}{2}}^{\frac{a}{2}} J_{zi}(x)\,E_{zi}(-x)\,dx = 0$$

In the above, $J_{zi}(x)$ is zero outside the strip, and $E_z(x)$ is zero on the strip. In this way, the final boundary condition is satisfied.

Equations (4) will be expressed in matrix form as follows:

$$\sum_{m=1}^{N} K_{im}^{(1,1)} C_m + \sum_{m=1}^{M} K_{im}^{(1,2)} d_m = 0, \qquad i = 1, 2, \ldots, N \qquad \text{(5a)}$$

$$\sum_{n=1}^{N} K_{in}^{(2,1)} C_n + \sum_{m=1}^{M} K_{in}^{(2,2)} d_n = 0, \qquad i = 1, 2, \ldots, M \qquad \text{(5b)}$$

where from the definition of the inner products associated with the Fourier transform defined by (2), the matrix elements are:

$$K_{im}^{(1,1)}(\omega_o) = \sum_{n=1}^{\infty} \sum_{m=1}^{\infty} \tilde{J}_{zi}(k_n, \beta_m)\,\tilde{Z}_{zz}\,\tilde{J}_{zm}(k_n, \beta_m) \qquad \text{(6a)}$$

$$K_{lm}^{(1,2)}(\omega_o) = \sum_{n=1}^{\infty}\sum_{m=1}^{\infty} \tilde{J}_{zl}(k_n, \beta_m)\,\tilde{Z}_{zx}\tilde{J}_{xm}(k_n, \beta_m) \tag{6b}$$

$$K_{lm}^{(2,1)}(\omega_o) = \sum_{n=1}^{\infty}\sum_{m=1}^{\infty} \tilde{J}_{xl}(k_n, \beta_m)\,\tilde{Z}_{xz}\tilde{J}_{zm}(k_n, \beta_m) \tag{6c}$$

$$K_{lm}^{(2,2)}(\omega_o) = \sum_{n=1}^{\infty}\sum_{m=1}^{\infty} \tilde{J}_{xl}(k_n, \beta_m)\,\tilde{Z}_{xx}\tilde{J}_{xm}(k_n, \beta_m) \tag{6d}$$

A homogeneous system of equations is thus obtained in terms of the unknown coefficients c_m and d_m. In order that c_m and d_m have nontrivial solutions, the determinant of the matrix must be zero, and hence the resonant frequency is determined for the resonator and discontinuity structures assumed.

Equations (5) are now solved for the resonant frequency ω_o by seeking the root of the resulting characteristic equation. The resonance frequency of the suspended stripline resonator is derived from the obtained value of ω_o[Eq.(8h)].

The accuracy of the solution can be systematically improved by increasing the number of basis functions (M,N) and by solving larger size matrix equations. However, if the first few basis functions are chosen so as to approximate the actual

unknown current distribution reasonably well, the necessary size of the matrix can be held small for a given accuracy of the solution, resulting in numerical efficiency. Hence the choice of basis functions is important from the numerical point of view.

B. GREEN'S FUNCTION FOR THE MOMENT METHOD

Equations (1a) and (1b) may be expressed in the matrix form:[Ref.2]

$$\begin{Vmatrix} \tilde{E}_z \\ \tilde{E}_x \end{Vmatrix} = \begin{Vmatrix} \tilde{Z}_{zz} & \tilde{Z}_{zx} \\ \tilde{Z}_{xz} & \tilde{Z}_{xx} \end{Vmatrix} \begin{Vmatrix} \tilde{J}_z \\ \tilde{J}_x \end{Vmatrix} \tag{7}$$

where the transformed Green's Functions have the values:

$$\tilde{Z}_{zz} = -\frac{1}{k_n^2+\beta_m^2}\left[\beta_m^2\tilde{Z}_e+k_n^2\tilde{Z}_h\right] \tag{8a}$$

$$\tilde{Z}_{xz} = \tilde{Z}_{zx} = -\frac{k_n\beta_m}{k_n^2+\beta_m^2}\left[\tilde{Z}_e-\tilde{Z}_h\right] \tag{8b}$$

$$\tilde{Z}_{xx} = -\frac{1}{k_n^2+\beta_m^2}\left[k_n^2\tilde{Z}_e+\beta_m^2\tilde{Z}_h\right] \tag{8c}$$

$$\tilde{Z}_e = \frac{\gamma_{y2}C_{t_1}+\gamma_{y1}C_{t_2}}{C_{t_1}C_{t_2}+C_{t_2}C_{t_3}\frac{\gamma_{y2}}{\gamma_{y1}}+C_{t_2}C_{t_3}\frac{\gamma_{y1}}{\gamma_{y2}}+\frac{\gamma_{y2}}{\gamma_{y2}}} \tag{8d}$$

$$\tilde{Z}_h = \frac{\gamma_{z2} C_{t_2} + \gamma_{z1} C_{t_1}}{\gamma_{z1}\gamma_{z2} C_{t_1} C_{t_2} + \gamma_{z1}\gamma_{z3} C_{t_1} C_{t_3} + \gamma_{z2}\gamma_{z3} C_{t_2} C_{t_3} + \gamma_{z2}^2} \qquad (8e)$$

where the symbols C_{t_i} have the values specified below:

case $\gamma_i^2 \geq 0$,

$$C_{t_1} = \coth \gamma_1 d, \quad C_{t_2} = \coth \gamma_2 t, \quad C_{t_3} = \coth \gamma_3 h \qquad (8f)$$

case $\gamma_i^2 < 0$,

$$C_{t_1} = -j \cot \gamma_1 d, \quad C_{t_2} = -j \cot \gamma_2 t, \quad C_{t_3} = -j \cot \gamma_3 h \qquad (8g)$$

where

$$\gamma_i = \sqrt{k_n^2 + \beta_m^2 - \mu_o \epsilon_i \omega^2} \qquad (8h)$$

$$\gamma_{yi} = \frac{\gamma_i}{j\omega\epsilon_i} \qquad (8i)$$

$$\gamma_{zi} = \frac{\gamma_i}{j\omega\mu_i} \qquad (8j)$$

where subscripts i refer to the i^{th} medium.

The quantities $\tilde{Z}_{zz}$, $\tilde{Z}_{zx}$, $\tilde{Z}_{xz}$, and $\tilde{Z}_{xx}$ are actually the Fourier transforms of dyadic Green's function components.

C. CHOICE OF RESONATOR FREQUENCY BELOW THE CUTOFF OF THE SHIELD ENCLOSURE

The cutoff frequency of the dielectric-loaded waveguide formed by the shielded SSSL shown in Fig.1 is found to be 5.73GHz, as calculated by the equation below [Ref.5].

$$f_c = \frac{c}{2a}\sqrt{1-\frac{t}{b}\frac{(\epsilon_r-1)}{\epsilon_r}} \qquad (9a)$$

where c is the velocity of light and the value of ε_r is 2.35. The dimensions a,b and t are defined in Fig. 1, and numerical values are shown in Table I.

TABLE I CONFIGURATION DATA

Dimension	Data	Dimension	Data
a	22.86 mm	t	1.59 mm
b	10.16 mm	h	4.285mm
w_1	5.00 mm	ε_r	2.35
d	4.285mm	RL	100.00 mm

Dimensions in Table I correspond to Fig.1 as follows:

a = Width of shield

b = Height of shield

d = Height of lower air layer

t = Thickness of dielectric substrate layer

h = Height of upper air layer

w_1 = Microstrip line width in continuity case

ε_r = Dielectric constant of substrate layer

RL = Length of shield

The effective dielectric constant and the frequency determine wavelength λ_g in the SSSL:

$$\lambda_g = \frac{c}{f\sqrt{\varepsilon_{eff}}} \qquad (9b)$$

where c is the velocity of light, f is the frequency, and ε_{eff} is the effective dielectric constant. Thus, $\lambda_g/2$ determines the fundamental resonance of the open ended length of strip, ℓ.

For simplicity, the strip is assumed to be symmetrically located, although the present method of analysis can be easily extended to more general cases. Also, the operating frequency is taken to be below cutoff of the shielding waveguide partially filled with substrate material, in order to avoid interaction of the strip transmission-line resonance with standing-wave resonances of the waveguide modes within the shielding enclosure.

D. EQUIVALENT NETWORK FOR A DISCONTINUITY IN A TRANSMISSION LINE SYSTEM: THE RESONATOR METHOD

In the resonator method for evaluating an equivalent circuit representation for a discontinuity in a transmission-line system, the discontinuity is placed at the approximate center of an open-ended strip of the transmission line.

Ignoring the end effect, the fundamental resonance of the unperturbed resonator strip occurs at a total resonator length of $\lambda_g/2$ of the guided wave length of the system. For this mode there is an current maximum at the center of the resonator [Fig. 2a]. The next higher resonance of the open-ended resonator occurs at a resonator length of λ_g, of the system wavelength [Fig. 2b].

In any event, if the line resonator is housed within a metallic shield, for example of waveguide cross-section, it is essential to choose a resonator length such that its resonance frequency is well below cutoff of the propagating modes of the waveguide system involved. This is a dielectric-loaded waveguide because of the presence of the dielectric substrate.

In the resonator method for determining the equivalent circuit representation of a discontinuity, the discontinuity is assumed to be lossless, and the equivalent circuit is regarded as a two-port circuit element acting as an impedance transformer between the two line-segments which make up the resonator[Fig. 3].

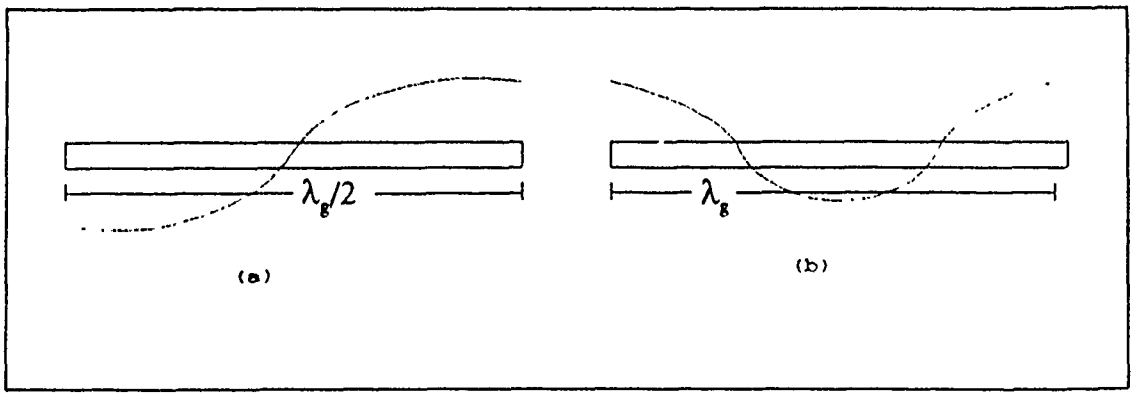

Figure 2 Resonance modes

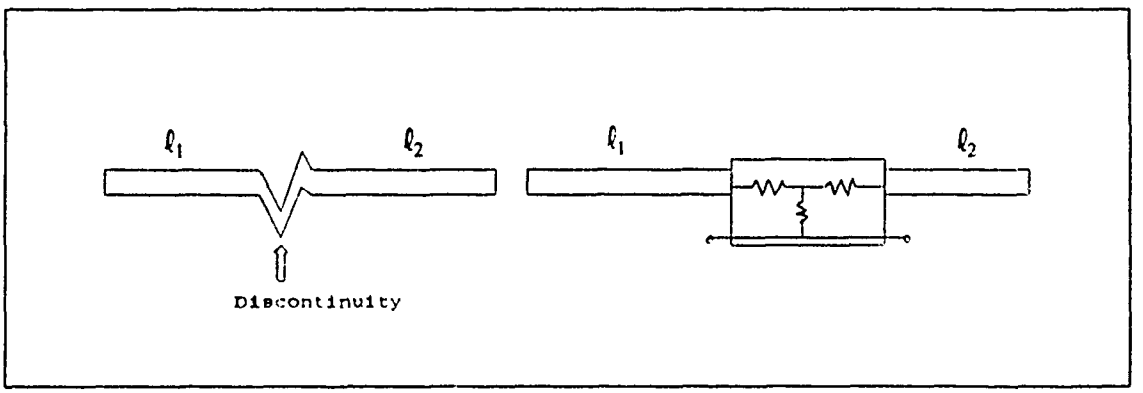

Figure 3 Impedances for line segments

Considering the resonator transmission line segment at the left of the two-port, the occurrence of resonance is specified by the condition:

$$z_1^* = z_{in1} \tag{10}$$

where the star means complex conjugate, z_1 is the impedance at the input of the open stub on the left, and z_{in1} is the impedance seen looking into the input at port

1. The two-port is terminated in the second open-ended line segment which makes up the remainder of the resonator[Fig. 4].

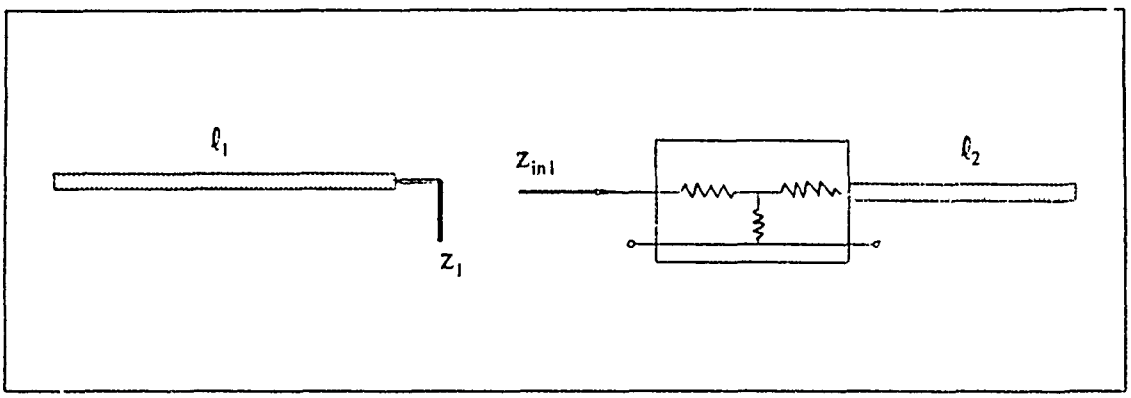

Figure 4 Equivalent-circuit expression for discontinuity

If the discontinuity under test is physically symmetrical about its center point, then it may be represented by a symmetrical T- or PI- circuit[Fig. 5]. However, for an asymmetrical discontinuity, such as for example the step change in width, the discontinuity may be represented by a general unsymmetrical T or PI, or an L-section if appropriate.

In the evaluation of the discontinuity by the resonance method, a pair of stub lengths ℓ_1 and ℓ_2 is chosen, of lengths appropriate to the test $(\ell_1+\ell_2)\cong\lambda_g/2$, or $(\ell_1+\ell_2)\cong\lambda_g$. The spectral domain model of the discontinuity is then employed to calculate the resonance frequency f_o of the resonator plus discontinuity. The terminating stub length ℓ_2 is changed by a small amount, and then the new length

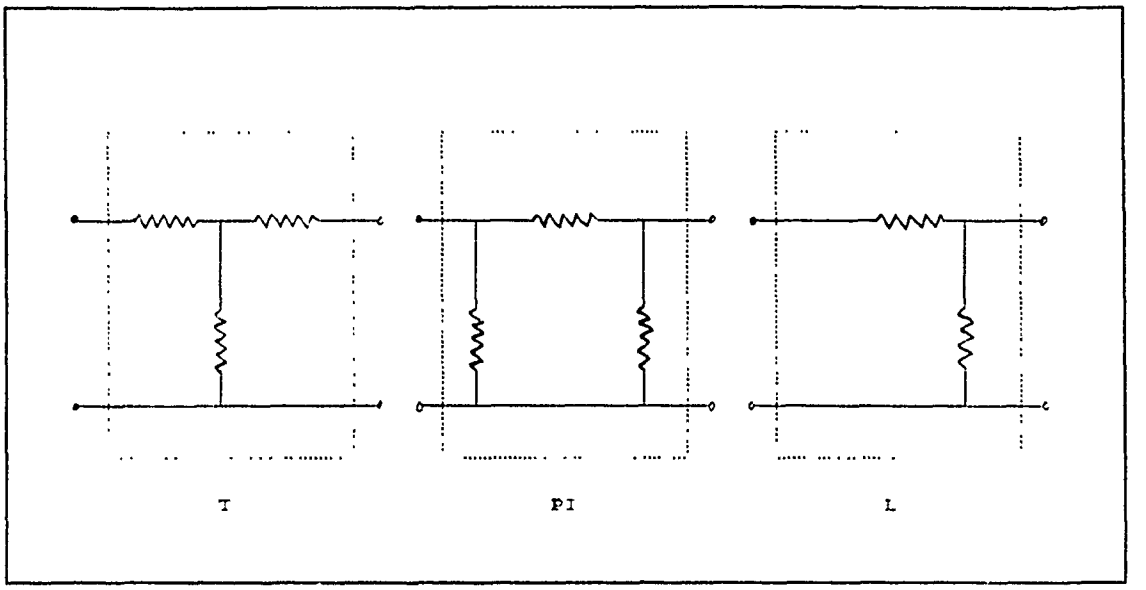

Figure 5 Presentations of Equivalent Circuits [Ref.6]

ℓ_1 of the stub at the input which is required to re-establish resonance at the same frequency f_o as above, is determined. This process is repeated until a sufficient number of stub-length pairs (ℓ_1,ℓ_2), which produce resonance at the same frequency f_o, is available for the calculation of the element values of the desired equivalent circuit representation.

In the case when an L-section equivalent circuit model is wanted, it turns out that, although only 2 independent circuit elements are included in the equivalent circuit, a determination of 3 pairs of (ℓ_1,ℓ_2) values is required, in order to effect separation of variables in the circuit equations. This is shown in section III.

Likewise, when an equivalent T- or PI-section presentation is evaluated for an asymmetrical discontinuity, a total of 4 of the (ℓ_1,ℓ_2) pairs must be resonated,

in order to provide the data needed for the determination of the 3 independent circuit elements in the equivalent circuit.

III. COMPUTER PROGRAM CONSTRUCTION

A. CURRENT DISTRIBUTIONS

In actual computations for the dominant mode, the strip current densities $\tilde{J}_{z1}$ and $\tilde{J}_{x1}$ have been chosen to have physically plausible distributions, as shown in Fig. 6, for the continuous strip which has width of $2w_1$ and length of 2ℓ.

1. Continuity Case

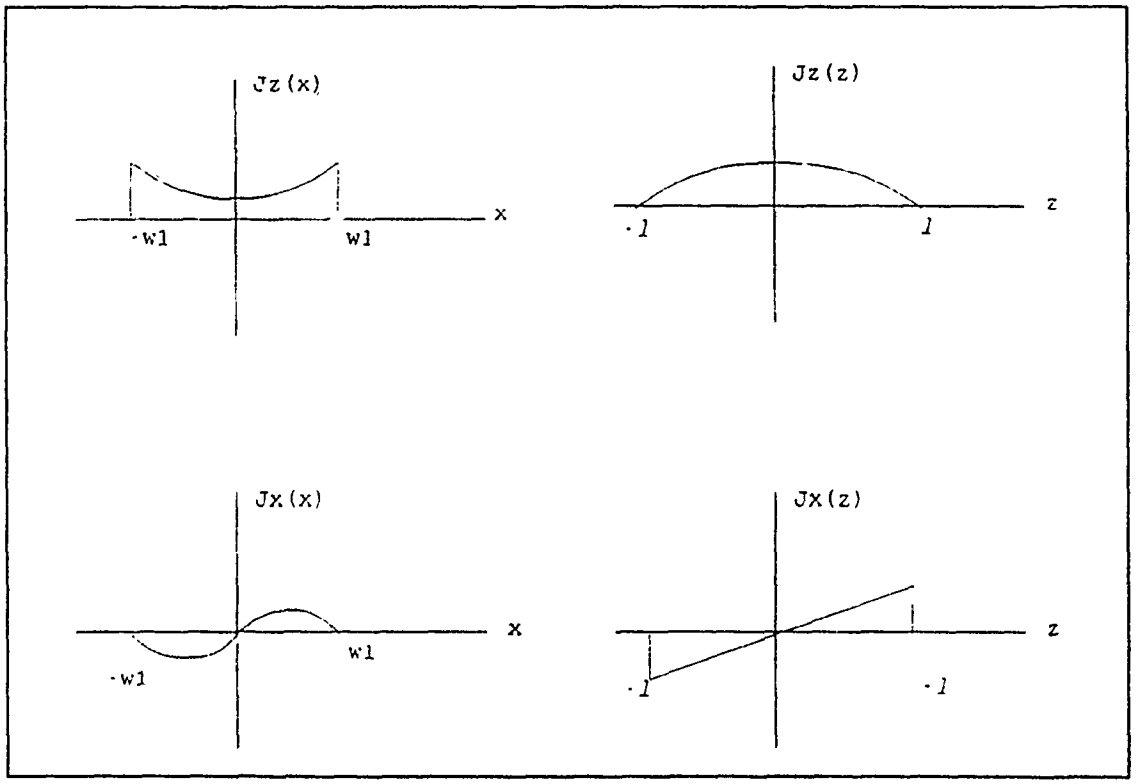

Figure 6 Forms of assumed current distributions

The coordinate forms of the current distributions in Fig. 6 are:

$$J_z(x) = \frac{1}{2W_1}\left[1+\left|\frac{x}{w_1}\right|^3\right] \tag{11a}$$

$$J_z(z) = \frac{1}{l}\cos\frac{\pi z}{2l} \tag{11b}$$

$$J_x(x) = \frac{1}{w_1}\sin\frac{\pi x}{w_1} \tag{11c}$$

$$J_x(z) = \frac{z}{2l^2} \tag{11d}$$

Fourier transforms of these are:

$$\tilde{J}_z(k_n) = \frac{2\sin(k_n w_1)}{k_n w_1} + \frac{3}{(k_n w_1)^2}[XIN] \tag{12a}$$

$$\left(XIN \equiv \cos(k_n w_1) - \frac{2\sin(k_n w_1)}{k_n w_1} + \frac{2[1-\cos(k_n w_1)]}{(k_n w_1)^2} \right)$$

$$\tilde{J}_z(\beta_m) = \frac{4\pi\cos\beta_m l}{\pi^2 - (2\beta_m l)^2} \tag{12b}$$

$$\tilde{J}_x(k_n) = \frac{2\pi\sin(k_n w_1)}{(k_n w_1)^2 - \pi^2} \tag{12c}$$

$$\tilde{J}_x(\beta_m) = \frac{\cos(\beta_m l)}{\beta_m l} - \frac{\sin(\beta_m l)}{(\beta_m l)^2} \tag{12d}$$

And then, forming products of the x- and z- dependent factors,

$$\tilde{J}_z(k_n, \beta_m) = \tilde{J}_z(k_n) \cdot \tilde{J}_z(\beta_m) \tag{13a}$$

$$\tilde{J}_x(k_n, \beta_m) = \tilde{J}_x(k_n) \cdot \tilde{J}_x(\beta_m) \tag{13b}$$

2. Step Discontinuity Case

If a step discontinuity is present at the approximate center of the microstrip line resonator, the simple current distributions shown in Fig. 7 are assumed within each line segment of fixed width for use in the computer program. The resonant frequencies can be computed and compared with the result for the continuous resonator.

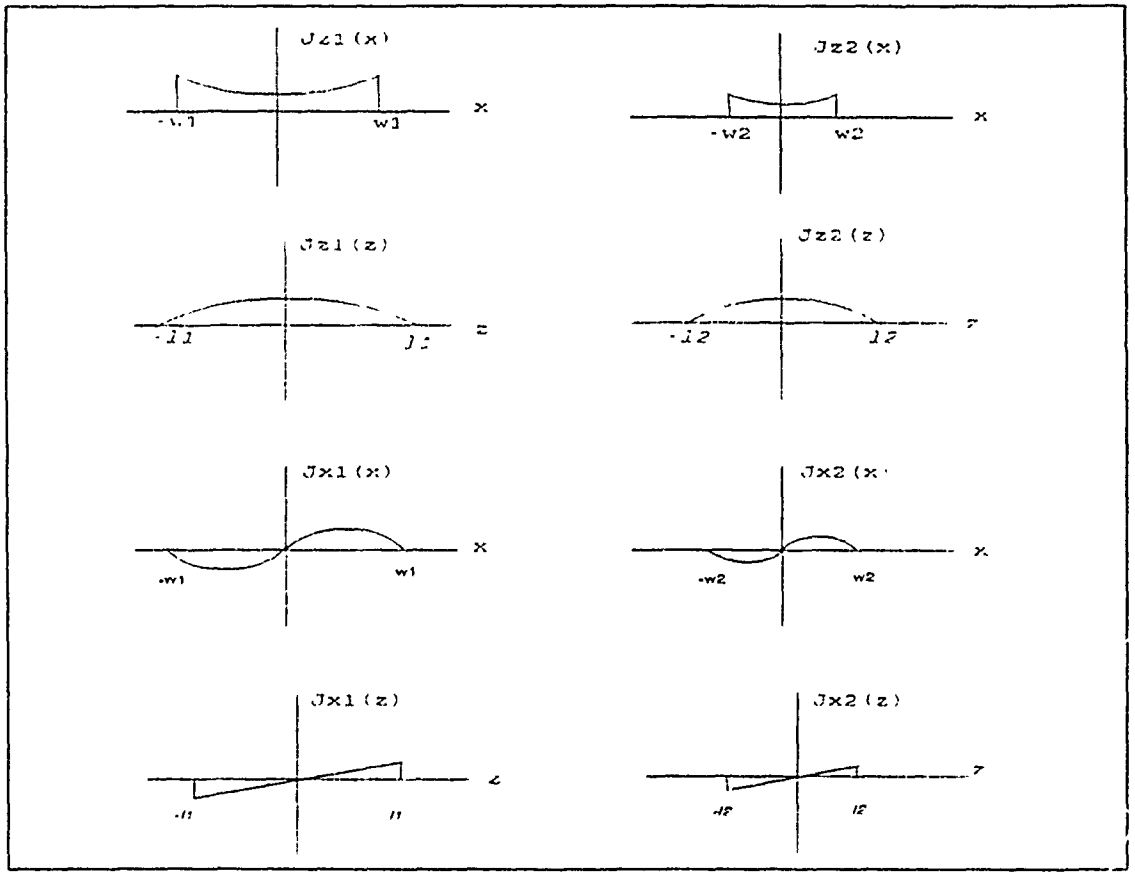

Figure 7 Forms of assumed current distribution with step discontinuity

The coordinate forms of current distributions in Fig. 7 are:

$$J_{z1}(x) = \frac{1}{2w_1}\left[1+\left|\frac{x}{w_1}\right|^3\right] \tag{14a}$$

$$J_{z2}(x) = \frac{1}{2w_2}\left[1+\left|\frac{x}{w_2}\right|^3\right] \tag{14b}$$

$$J_{z1}(z) = \frac{1}{l_1}\cos\frac{\pi z}{2l_1} \tag{14c}$$

$$J_{z2}(z) = \frac{1}{l_2}\cos\frac{\pi z}{2l_2} \tag{14d}$$

$$J_{x1}(x) = \frac{1}{w1}\sin\frac{\pi x}{w_1} \tag{14e}$$

$$J_{x2}(x) = \frac{1}{w_2}\sin\frac{\pi x}{w_2} \tag{14f}$$

$$J_{x1}(z) = \frac{z}{2l_1^2} \tag{14g}$$

$$J_{x2}(z) = \frac{z}{2l_2^2} \tag{14h}$$

The Fourier transformed distributions of Eqs. (15) are:

$$\tilde{J}_{z1}(k_n) = \text{Same as Eq. (12a)} \tag{15a}$$

$$\tilde{J}_{z2}(k_n) = \frac{2\sin(k_n w_2)}{k_n w_2} + \frac{3}{(k_n w_2)^2}[XIN] \tag{15b}$$

$$\left(XIN \equiv \cos(k_n w_2) - \frac{2\sin(k_n w_2)}{k_n w_2} + \frac{2[1-\cos(k_n w_2)]}{(k_n w_2)^2} \right)$$

$$\tilde{J}_{z1}(\beta_m) = \text{Same as Eq. (12b)} \tag{15c}$$

$$\tilde{J}_{z2} = \frac{4\pi\cos(\beta_m l_2)}{\pi^2 - (2\beta_m l_2)^2} \tag{15d}$$

$$\tilde{J}_{x1}(k_n) = \text{Same as Eq. (12c)} \tag{15e}$$

$$\tilde{J}_{x2}(k_n) = \frac{2\pi\sin(k_n w_2)}{(k_n w_2)^2 - \pi^2} \tag{15f}$$

$$\tilde{J}_{x1}(\beta_m) = \text{Same as Eq. (12d)} \tag{15g}$$

$$\tilde{J}_{x2}(\beta_m) = \frac{\cos(\beta_m l_2)}{\beta_m l_2} - \frac{\sin(\beta_m l_2)}{(\beta_m l_2)^2} \tag{15h}$$

In Eq.(4), the case of M=N=2 is employed below. Therefore,

$$\tilde{J}_{z2}(k_n, \beta_m) = d_1 \tilde{J}_{z1}(k_n) \cdot \tilde{J}_{z1}(\beta_m) + d_2 \tilde{J}_{z2}(k_n) \cdot \tilde{J}_{z2}(\beta_m) \tag{16a}$$

$$\tilde{J}_{x2}(k_n, \beta_m) = c_1 \tilde{J}_{x1}(k_n) \cdot \tilde{J}_{x1}(\beta_m) + c_2 \tilde{J}_{x2}(k_n) \cdot \tilde{J}_{x2}(\beta_m) \tag{16b}$$

where the individual terms have non-zero values only in the line segment indicated by the corresponding subscript, as explained above.

From Eqs. (5) and (6)

$$K11 = \sum_{n=1}^{\infty} \sum_{m=1}^{\infty} \tilde{J}_{z1}(k_n, \beta_m) \tilde{Z}_{zz} \tilde{J}_{z1}(k_n, \beta_m) \tag{17a}$$

$$K12=\sum_{n=1}^{\infty}\sum_{m=1}^{\infty}\tilde{J}_{z1}(k_n,\beta_m)\,\tilde{Z}_{zx}\tilde{J}_{x1}(k_n,\beta_m) \tag{17b}$$

$$K21=\sum_{n=1}^{\infty}\sum_{m=1}^{\infty}\tilde{J}_{x1}(k_n,\beta_m)\,\tilde{Z}_{xz}\tilde{J}_{z1}(k_n,\beta_m) \tag{17c}$$

$$K22=\sum_{n=1}^{\infty}\sum_{m=1}^{\infty}\tilde{J}_{x1}(k_n,\beta_m)\,\tilde{Z}_{xx}\tilde{J}_{x1}(k_n,\beta_m) \tag{17d}$$

B. COMPUTATION PROCEDURES

1. Change of Transform Variable

In the present work, the strip line resonator was fully enclosed in a metal shield. This permitted the use of a finite Fourier transform rather than the integral transform which is typical of the infinite-line calculations.

The inner products can then be carried out as truncated summations, saving much computer time[Ref.9].

$$\sum_{n=1}^{\infty}\int_{0}^{\infty} \rightarrow \sum_{n=1}^{\infty}\sum_{m=1}^{\infty}$$

Strictly speaking, the limits are n=-∞, m=-∞ on the low side, unless symmetry holds, and the sum is:

$$2\cdot\sum_{m=1}^{\infty} = \sum_{m=-\infty}^{\infty}$$

The wavenumbers used for the two summations are:

$$k_n = \frac{(n-\frac{1}{2})\pi}{a}, \quad x\text{-direction}$$

$$\beta_m = \frac{(m-\frac{1}{2})\pi}{RL}, \quad z\text{-direction}$$

As shown on Table II and III, a summation over n of 20 terms is enough, and for the summation over m, 100 terms leads to convergence within 1 MHz error which is negligible in comparison with the resonant frequency.

TABLE II VARIATION OF NUMBER OF TERMS N

n	m	f_o (GHz)
10	100	5.7168
20 *	100	5.7250
40	100	5.7261

TABLE III VARIATION OF NUMBER OF TERMS M

n	m	f_o (GHz)
20	40	5.7072
20	80	5.7228
20	100 *	5.7250
20	200	5.7275

2. Equations for Some Factors

a. Propagation Constant β

By use of the program shown in Appendix A, β is computed at each resonant frequency and line-width w_1 and w_2. This program is constructed using the moment method of calculation.

b. Effective Dielectric Constant

The calculation of ϵ_{eff} uses $\beta(f)$, frequency-dependent propagation constant, and β_{air}, quasi-static propagation constant [Ref.3].

$$\epsilon_{eff} = \left[\frac{\beta(f)}{\beta_{air}}\right]^2 \qquad (18)$$

c. Characteristic Impedance $Z_o(f)$

The computation of characteristic impedance uses an empirical calculation for the quasistatic value, $Z_o(0)$ which has been confirmed to be accurate [Ref.10]. This value is then corrected to the wanted frequency f by use of ϵ_{eff} in the expression :[Ref.4]

$$Z_o(f) = \frac{Z_o(0)}{\sqrt{\epsilon_{eff}}} \qquad (19)$$

for $0 < w < a/2$;

$$Z_o(0) = 60\left[V + R \cdot \ln\left[\, 6\frac{b}{w} + \sqrt{1+4\left(\frac{b}{w}\right)^2}\,\right]\right]$$

$$V = -1.7866 - 0.2035(t/b) + 0.4750(a/b)$$

$$R = 1.0835 + 0.1007(t/b) - 0.09457(a/b)$$

for $a/2 < w < a$;

$$Z_o(0) = 120\pi\left[V + R\left[\frac{w}{b} + 1.3930 + 0.6670 \cdot \ln\left(\frac{w}{b} + 1.444\right)\right]^{-1}\right]$$

$$V = -0.6301 - 0.07082(t/b) + 0.2470(a/b)$$

$$R = 1.9492 + 0.1553(t/b) - 0.5123(a/b)$$

C. PRESENTATION OF THE L-CIRCUIT COMPONENTS WHICH REPRESENT THE DISCONTINUITY

The network is considered as a two-port, i.e., 4-terminal, element terminated in open-ended stub sections, as indicated in Fig. 8.

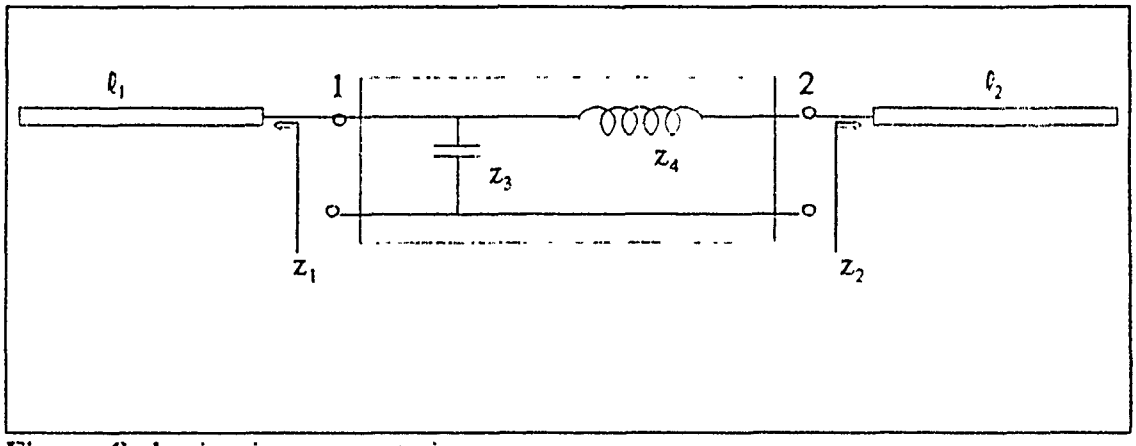

Figure 8 L-circuit representation

The impedance at the input to port 1 is z_{in1}. The two stubs have input impedances:

$$z_1 = -jz_{01}\cot\beta_1 l_1 \qquad (20a)$$

$$z_2 = -jz_{02}\cot\beta_2 l_2 \qquad (20b)$$

The input impedance to the network is then:

$$z_{in1} = \frac{z_3 (z_4 + z_2)}{z_2 + z_3 + z_4} \tag{21}$$

Setting $z_{in1} = z_1^*$, and expanding the expression, we get:

$$z_3 A - z_3 z_4 + z_4 B = C \tag{22a}$$

where we define: $A \equiv z_1^* - z_2$

$B \equiv z_1^*$

$C \equiv -z_1^* z_2$

We now assume that we have values A, B, C and A',B',C', as well as A",B",C", of the constants defined above, corresponding to different stub-length pairs, (ℓ_1, ℓ_2), (ℓ_1', ℓ_2'), and (ℓ_1'', ℓ_2''), all of which have been determined by spectral-domain calculations to resonate at the same resonance frequency f_o.

We rewrite the equation above for each of the stated cases:

$$z_3 A' - z_3 z_4 + z_4 B' = C' \tag{22b}$$

$$z_3 A'' - z_3 z_4 + z_4 B'' = C'' \tag{22c}$$

Eqs.(22) are solved simultaneously to obtain the values for the circuit components z_3 and z_4:

$$z_3 = \frac{(C-C'')\,(B-B') - (C-C')\,(B-B'')}{(A-A'')\,(B-B') - (A-A')\,(B-B'')} \qquad (23a)$$

$$z_4 = \frac{(C-C') - z_3\,(A-A')}{(B-B')} \qquad (23b)$$

The component values for a three-element PI- or T-circuit can be calculated in a completely analogous manner, but with use of a set of four (ℓ_1,ℓ_2) pairs.

D. RESULTS OF COMPUTATION

1. Strip Resonator with Uniform Width

a. Resonant Frequencies with Varying Height of Lower Air Layer

The lower air gap is varied from the bottom of the shield to the middle of the shield height. When the dielectric material is near the bottom, comparable to the case of the microstrip line configuration, the resonant frequencies of SSSL show the same dependence on width w_1 as for a microstrip resonator [Ref.1]. As the air gap becomes larger, the tendency is reversed[Fig.9].

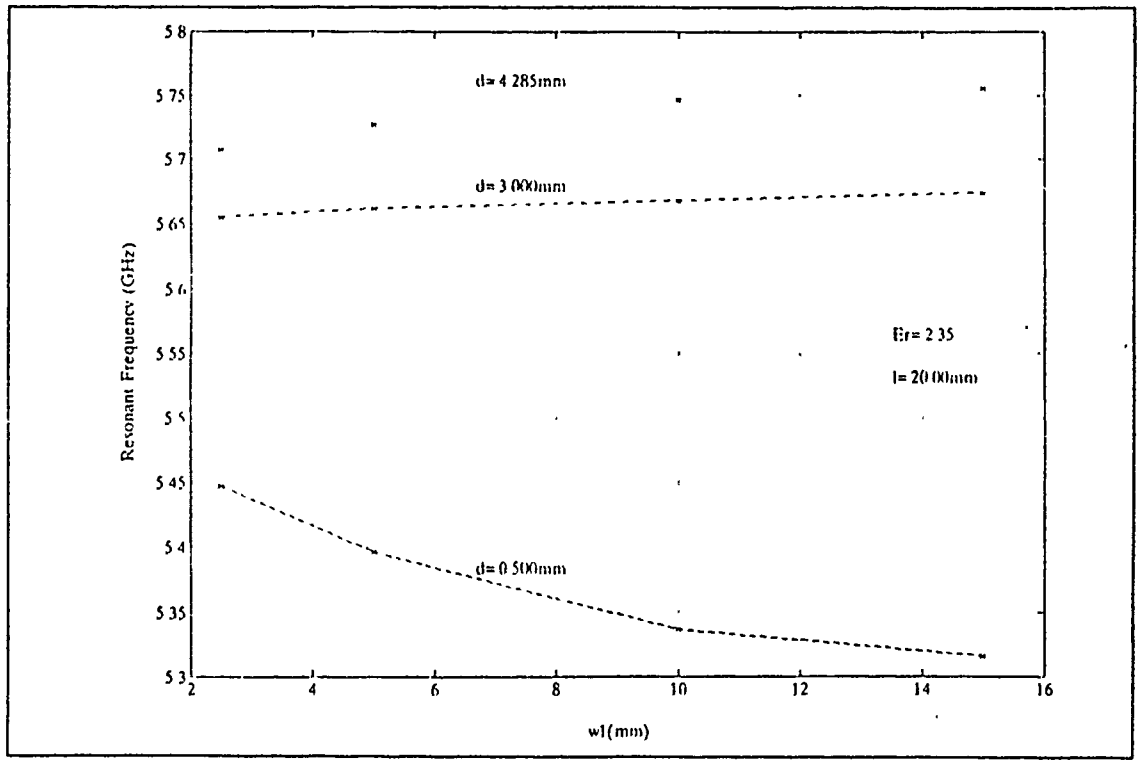

Figure 9 Resonant frequency vs. width of strip with change of lower air gap

b. Resonant Frequencies with Varying Lengths of Stub Segments on the Test Resonator

When the length of strip is greater, the resonant frequency is smaller as expected, because the resonant wavelength is proportional to the length of strip.

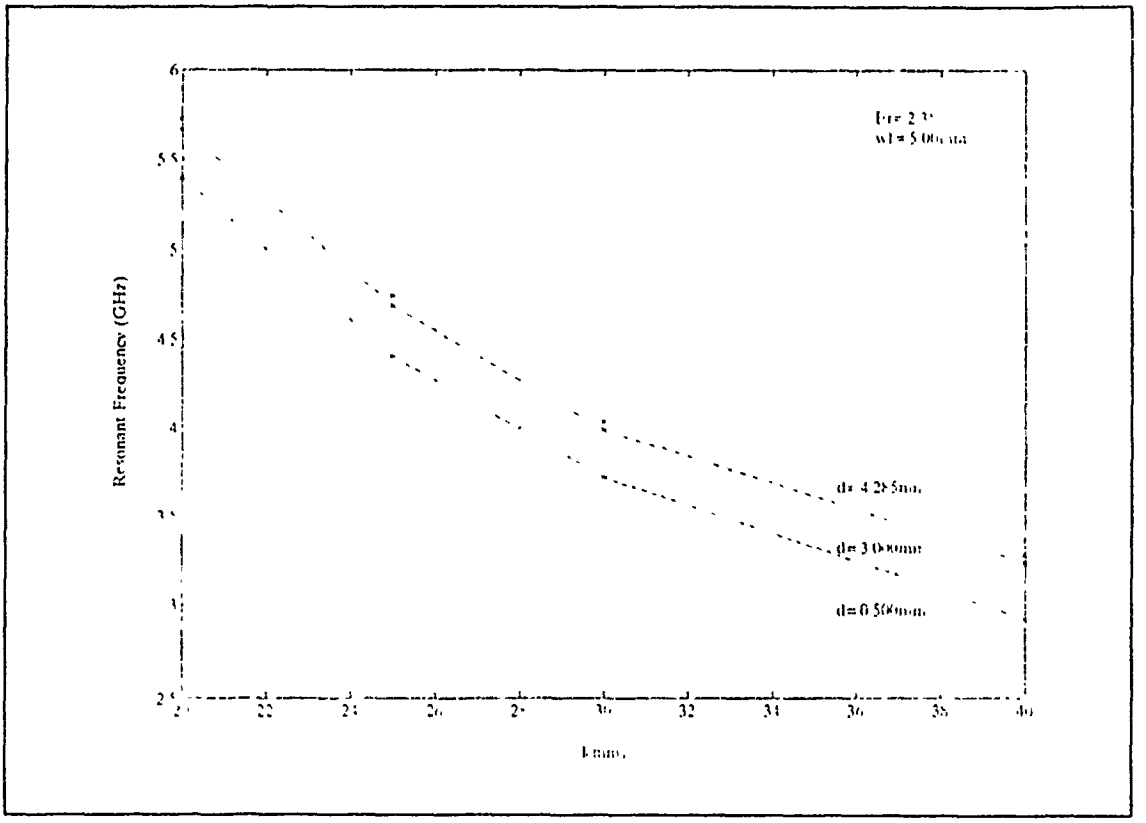

Figure 10 Resonant frequency vs. length of strip with change of lower air gap

c. *Effects of Change of Substrate Dielectric Constant*

As the substrate dielectric constant is increased, the resonant frequency of the strip resonator is reduced. But the variation of resonant frequency with change of lower air gap is faster as dielectric constant increases[Fig.11].

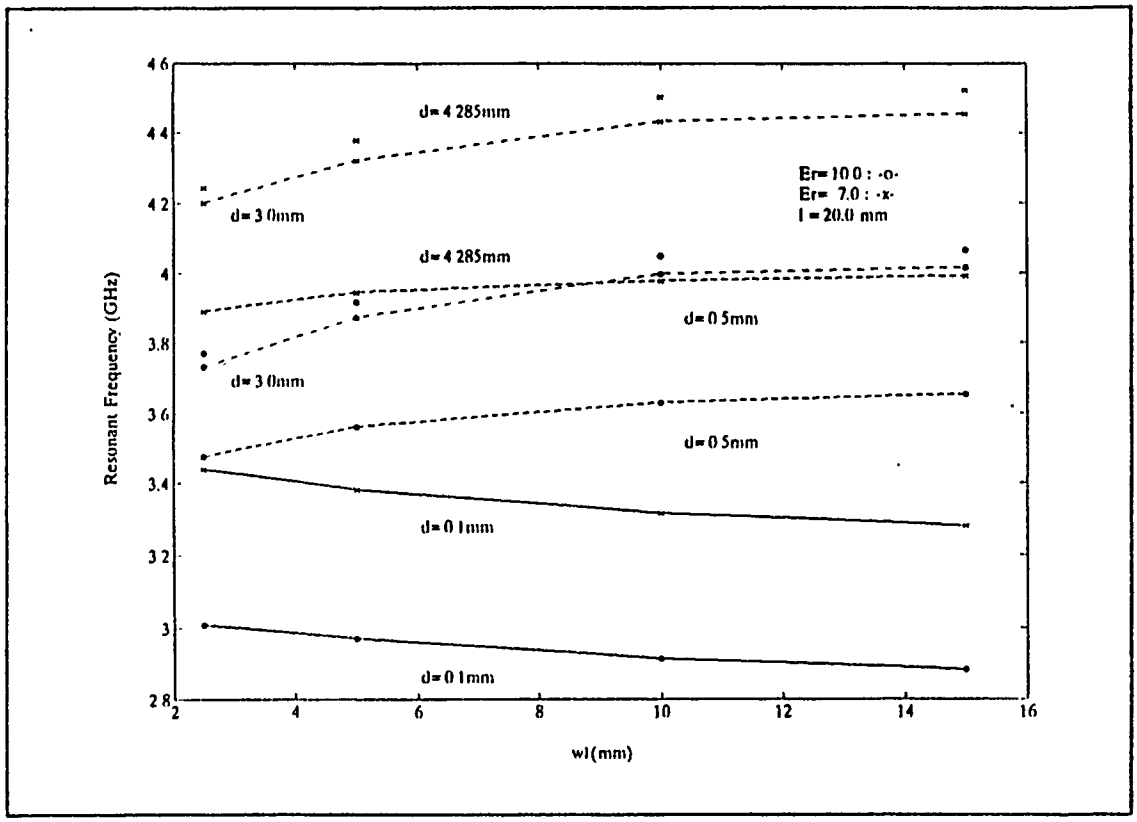

Figure 11 Resonant frequency vs. width of strip with change of ε_r

2. Strip Resonator with Step Discontinuity in Width

a. Resonant Frequencies with Discontinuity at Center of Resonator

When the length $\ell_1(=\ell_2)$ is decreased, the resonant frequency is increased as in the uniform width resonator shown in Fig. 10. A greater difference between widths w_1 and w_2 results in a larger decrease of resonant frequency.

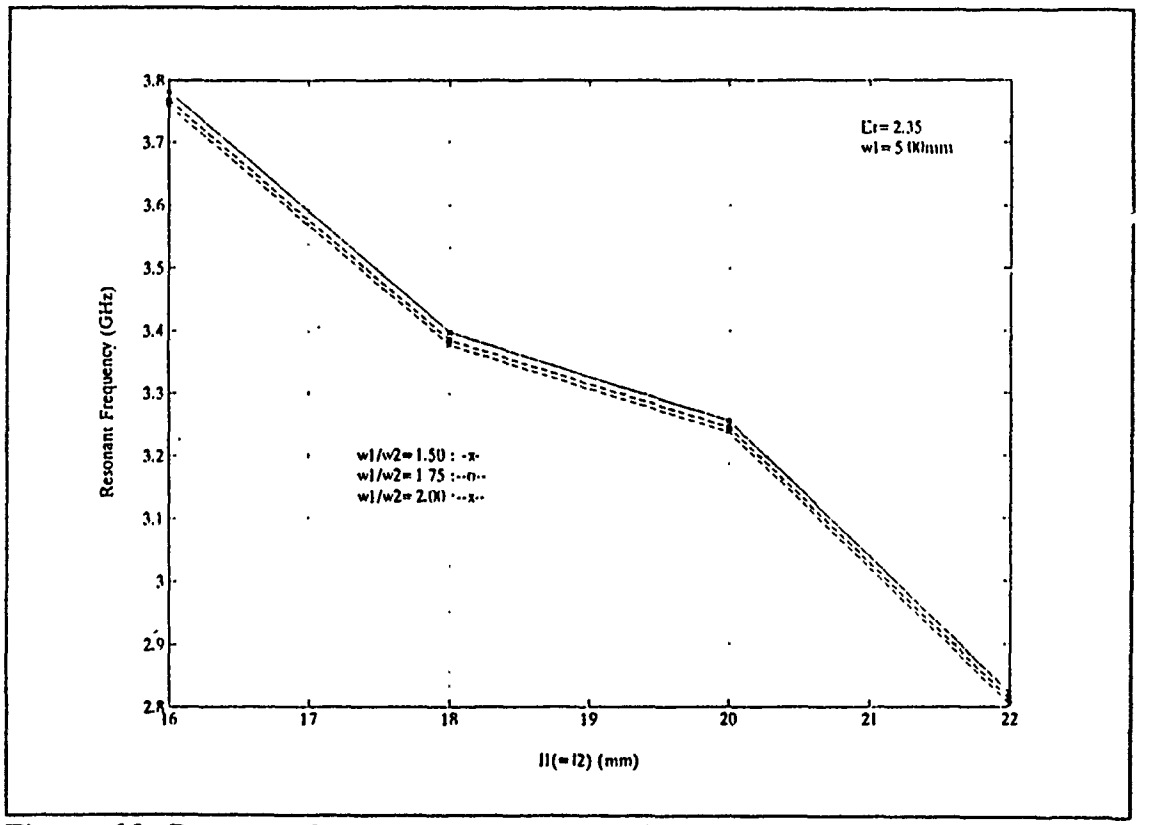

Figure 12 Resonant frequency vs. $\ell_1(=\ell_2)$ with different w_1/w_2

b. Resonant Frequencies with Varying Ratio of Lengths

A change of the ratio of the lengths affects the resonant frequencies. In turn, the greater difference between the lengths of the segments of different widths the higher is the resonator frequency. However, the resonant frequency converged to a single value, as the ratio of two lengths is was made larger.

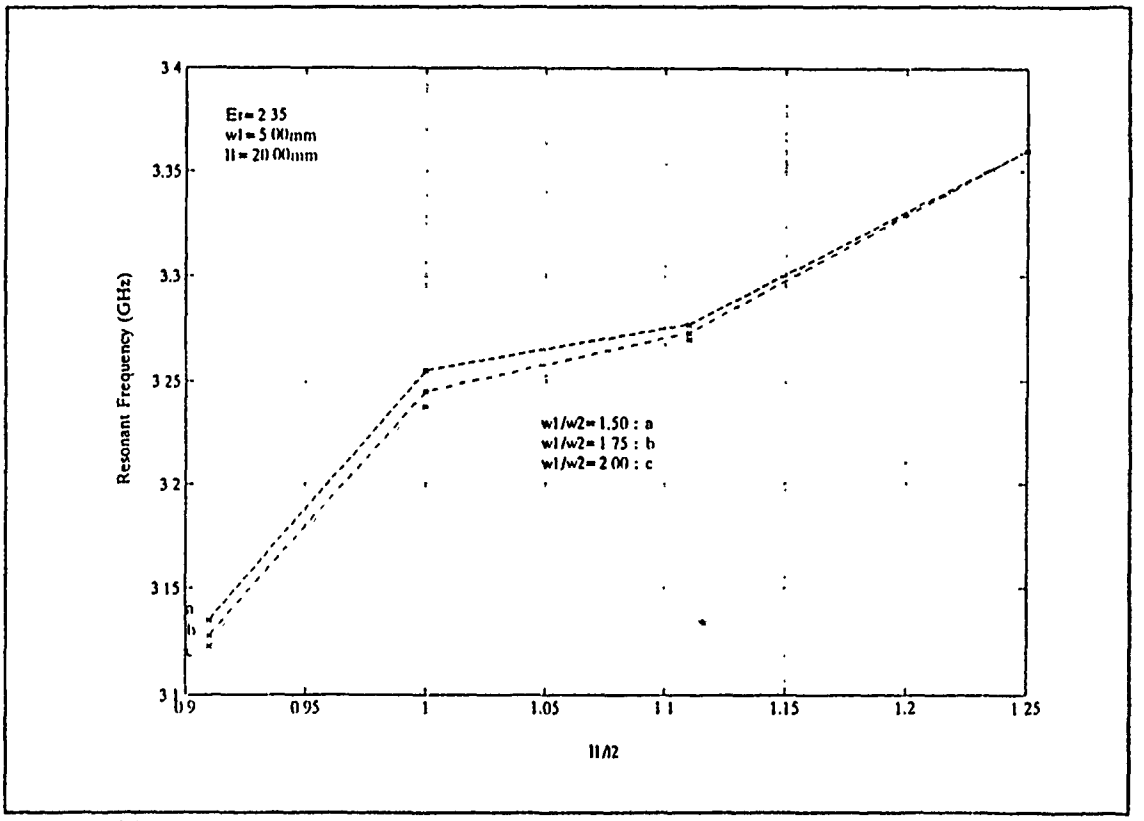

Figure 13 Resonant frequency vs. ℓ_1/ℓ_2 with different w_1/w_2

c. *Capacitance of Step with varying Parameters*

The equivalent-circuit capacitance of Fig.8 is dependent on the resonant frequency. To get the different resonant frequencies the length of stub, $\ell_1(=\ell_2)$, is changed. When ℓ_2 becomes shorter, there is corresponding ℓ_1 which produces resonance with the same frequency as the reference case. As mentioned before, 3 pairs of (ℓ_1, ℓ_2) are needed. Here, the reference case,$\ell_1=\ell_2$, can not be one of the three because it was found that using this case resulted in negative values of capacitance resulting from the computation. More investigation is required to determine the reason for this behavior.

As shown in Fig.14 & Fig.15, a greater value of the ratio w_1/w_2 corresponds to a greater value of discontinuity capacitance, as expected[Ref.7]. However, when the w_1/w_2 approaches to unity, the capacitance does not decrease continuously but was found to increase. Since the limiting case, $w_1/w_2=1$, should correspond to zero capacitance, the result obtained seems to be due to the fact that the difference terms in Eq.(23) represent the taking of differences between nearly-equal quantities, and a small error in the individual quantities will produce a large error in the result. Other factors are the approximate nature of the basis functions and/or the small number of basis functions.

Shorter values of ℓ_1 and ℓ_2 correspond to higher resonant frequency. The variation of resonant frequency shows the frequency-dependence of the

equivalent- circuit capacitance [Fig.16]. Also, a greater substrate dielectric constant corresponds to a greater equivalent-circuit capacitance as expected on physical grounds [Fig.17].

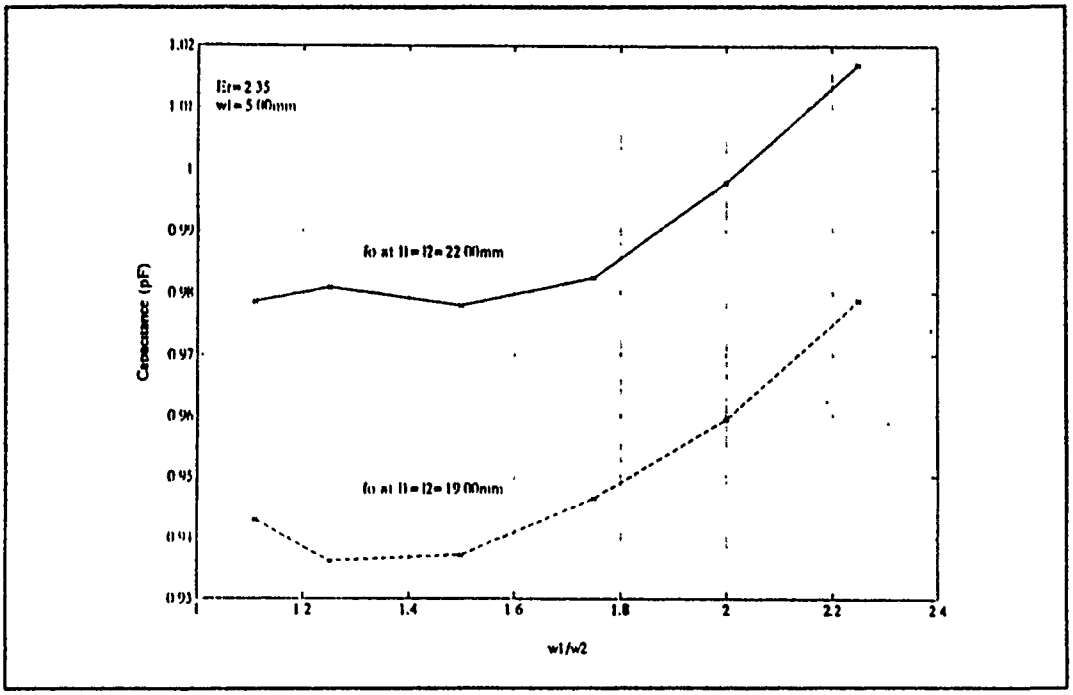

Figure 14 Capacitance vs. w_1/w_2 with change of initial resonator length

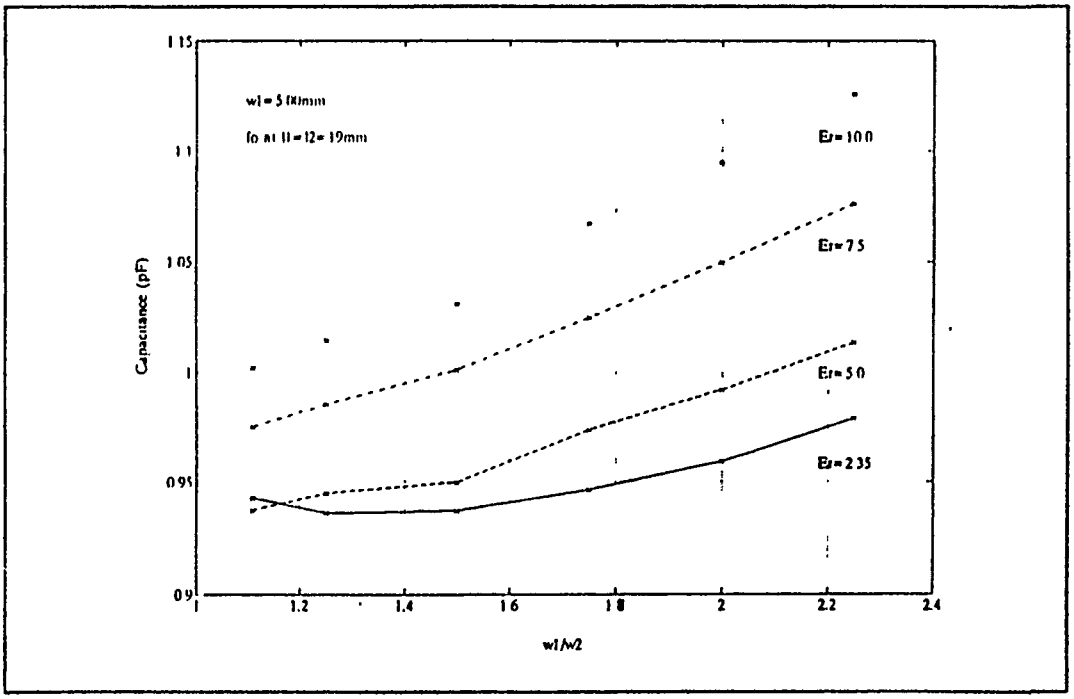

Figure 15 Capacitance vs. w_1/w_2 with change of ε_r

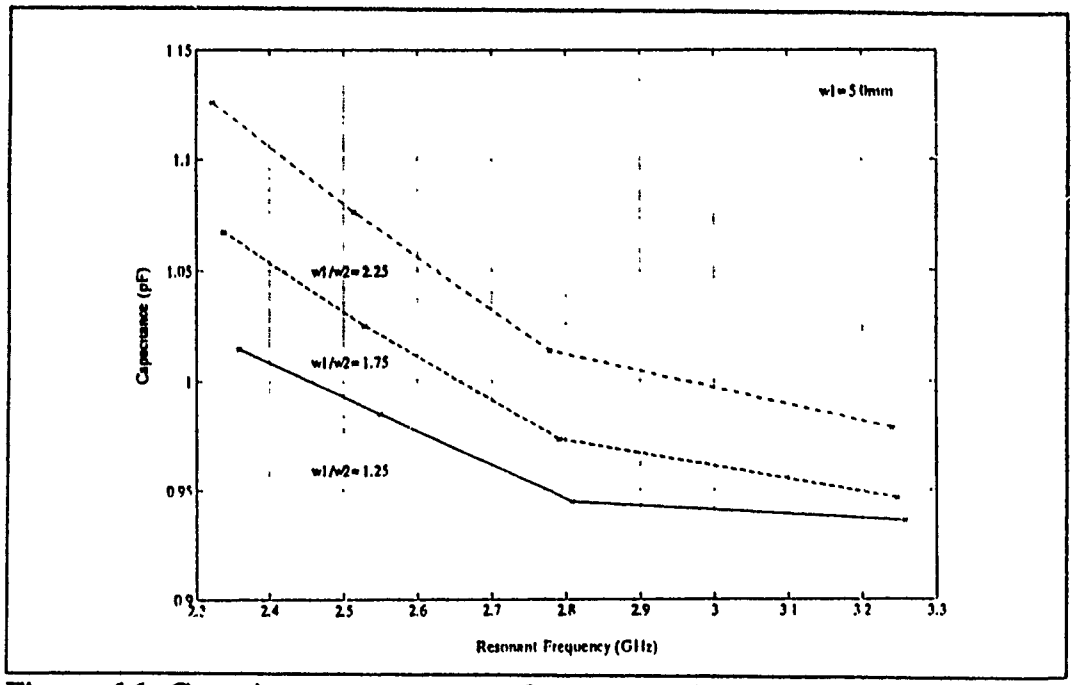

Figure 16 Capacitance vs. resonant frequency with change of w_1/w_2

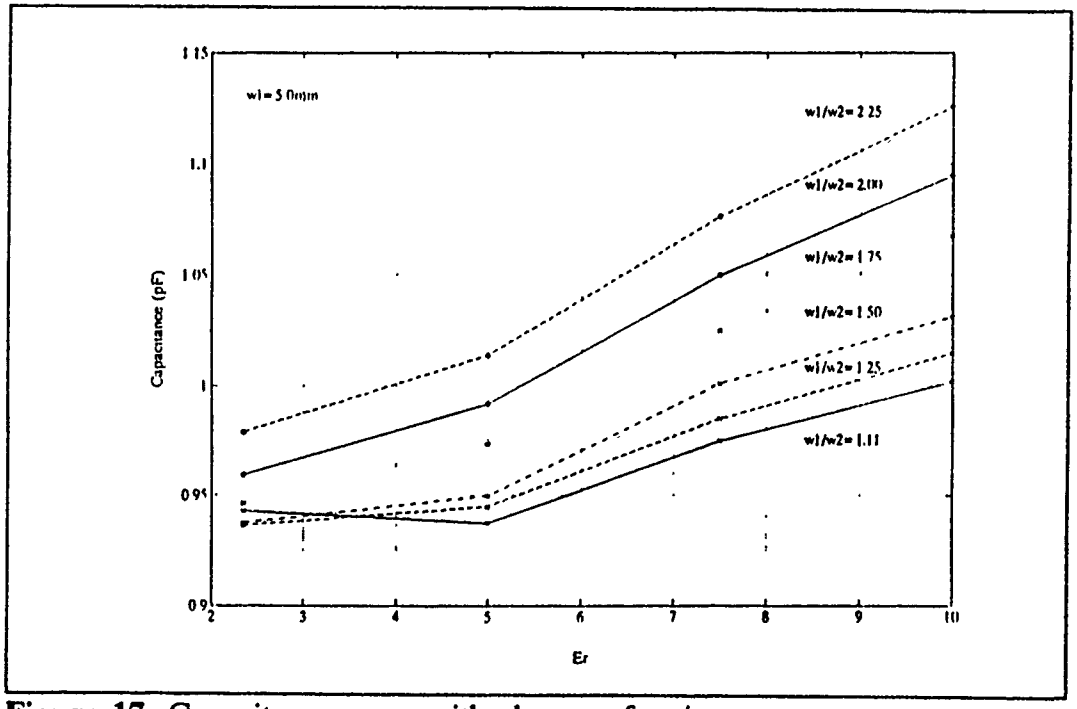

Figure 17 Capacitance vs. ε_r with change of w_1/w_2

d. Inductance of Step with varying Parameters

The procedure for the calculation of the equivalent circuit inductance is analogous to that used in the case of the capacitance. The calculated inductance did not converge to zero when w_1/w_2 goes to unity, also[Ref.8]. The inductance does not show a monotonic increase for w_1/w_2 greater than two[Fig. 18]. This seems to be due to the approximate nature of the calculation.

Fig.19 generally shows similar behavior of the calculated inductance, with several different values of dielectric constant. The inductance decreases as the resonant frequency increases, however[Fig.20]. Increasing the substrate dielectric constant causes a uniform increase in the discontinuity inductance[Fig.21].

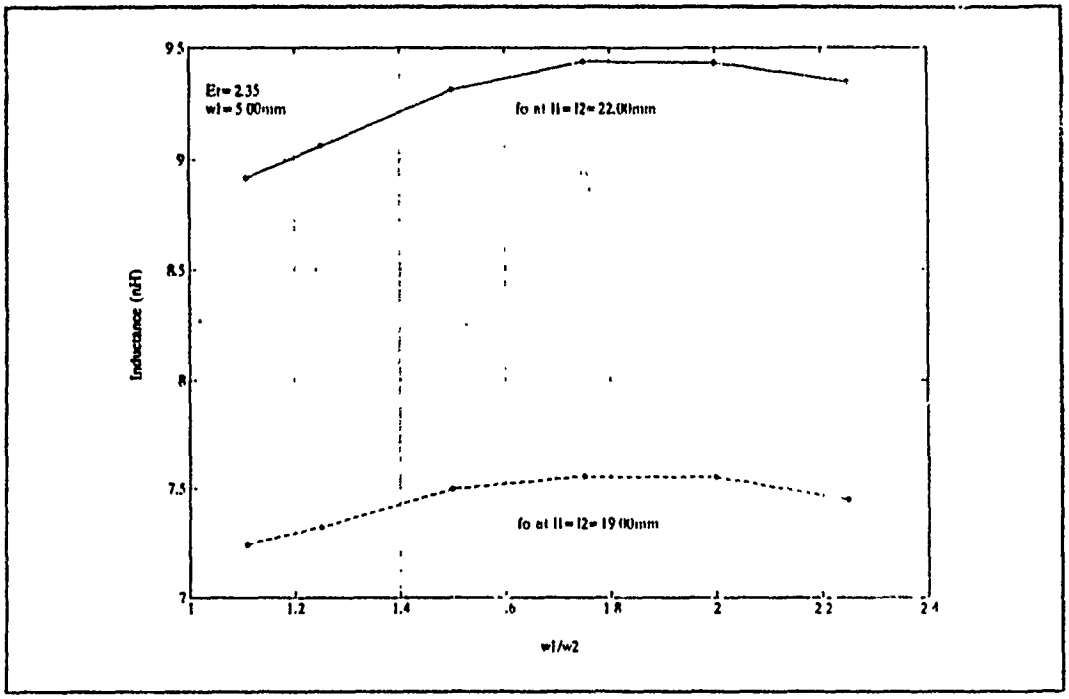

Figure 18 Inductance vs. w_1/w_2 with change of initial resonator length

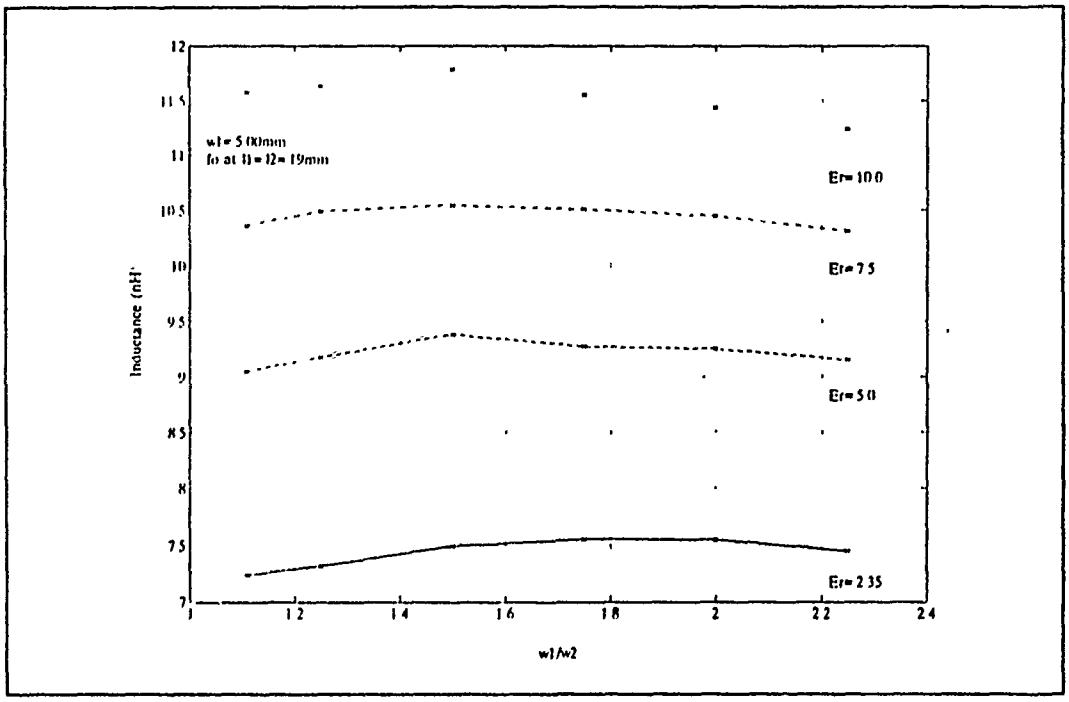

Figure 19 Inductance vs. w_1/w_2 with change of ε_r

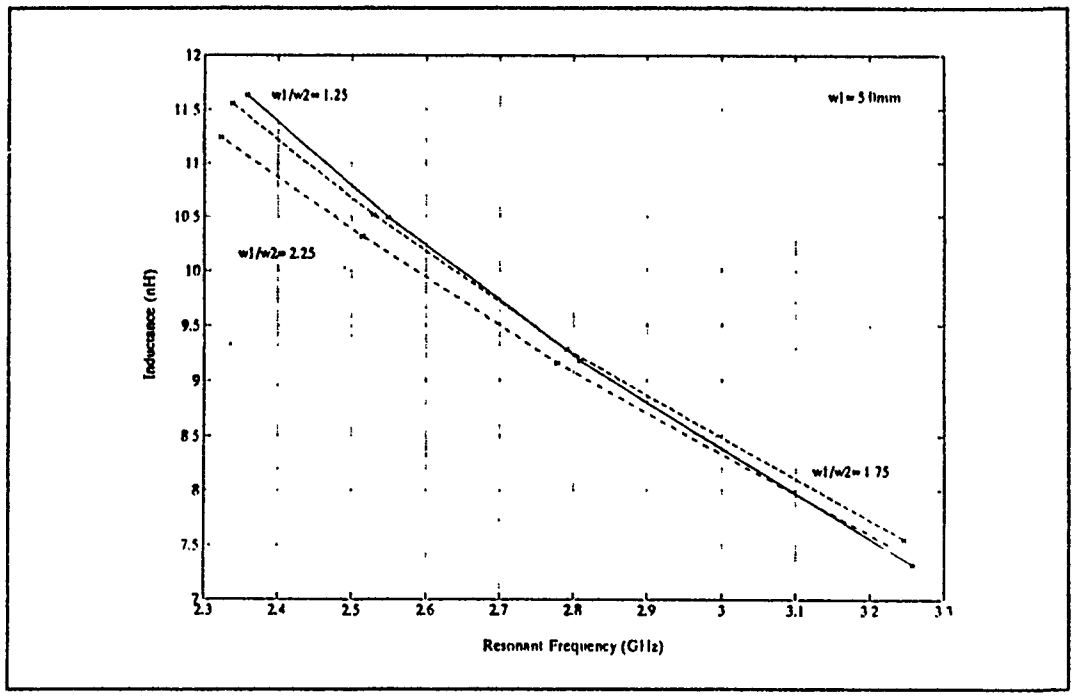

Figure 20 Inductance vs. resonant frequency with change of w_1/w_2

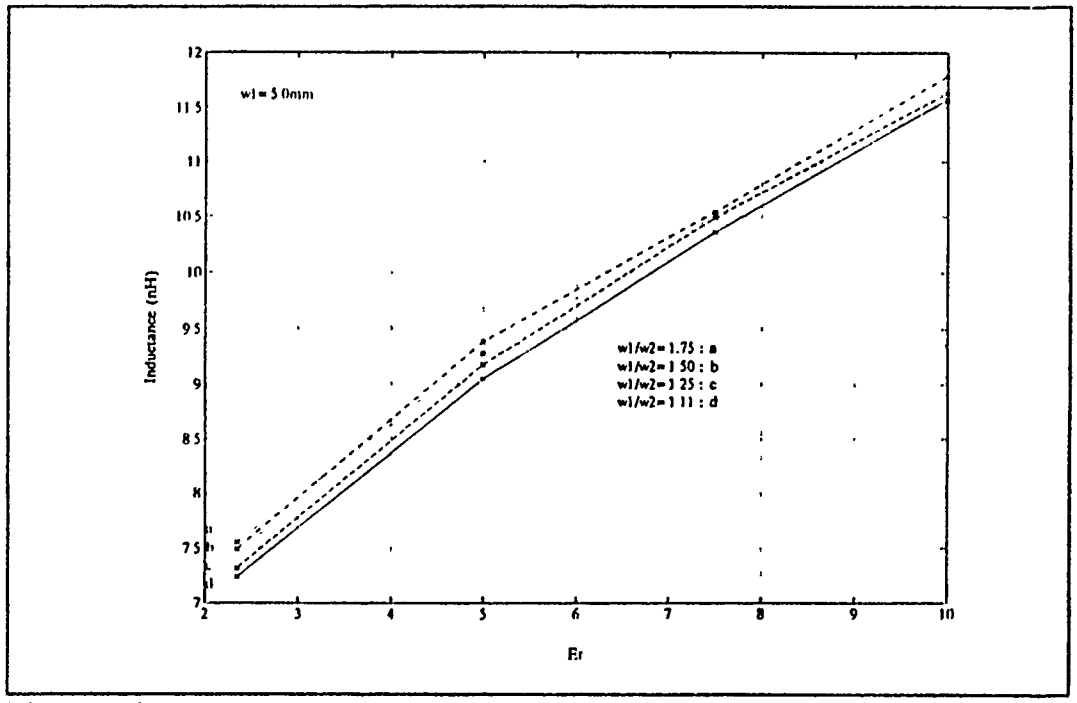

Figure 21 Inductance vs. ε_r with change of w_1/w_2

IV. CONCLUSION

This thesis follows the methods originated by Itoh for the analysis of the shielded suspended stripline resonator[Ref.1 & 3]. A fully-shielded enclosure was employed, allowing the use of a finite Fourier transform in two coordinate directions. This change reduced the computation time significantly, while producing accuracy comparable with that of the use of the integral transform along the line axis.

The perturbed-resonator technique permitted the use of the strip current-density distributions suggested by Itoh[Ref.1]. These are known to give accurate results in Galerkin's method.

We may assume various functional forms for the current distribution on the line-stub of the resonator. However, no single distribution can give an exact result, though a larger number of distribution functions should lead to more accurate results. The choice of distribution function is important because of the very small number of functions used in this work.

The data of Fig.9 shows an interesting change of the slope of the resonant frequency vs width ratio with varying height of lower air gap[Fig.1]. Fig.14 & 18 shows increasing of capacitance and inductance respectively, as the resonant frequency decreases. But, as mentioned above, these graphs show some deviation

from expectation, in that the capacitance and inductance values fail to become zero with no step in width. This behavior should be given further research.

APPENDIX. COMPUTER PROGRAMS USING FORTRAN

A. RESONANT FREQUENCY

```
FILE: STEPF0   FOR      A1

      INTEGER I,N,M,COMPARE,COUNT
      REAL*8   W1,W2,L1,L2,A,D,T,H,ER,F
      REAL*8   KN,BETA,OMEGA,RL,RRL
      REAL*8   PI,E0,MU0,C
      REAL*8   GAM1S,GAM2S
      REAL*8   JZIN1,JZIN2,JZKN1,JZBE1,JXKN1,JXBE1,JX1,JZ1
      REAL*8   JZKN2,JZBE2,JZBE3,JXKN2,JXBE2
      REAL*8   CMP,LIMIT,OLDF,NEWF,LIMF
C
      LOGICAL LLOG
C
      COMPLEX*16  GAMA1,GAMA2,GAMA3,CT1,CT2,CT3
      COMPLEX*16  ZEN,ZENR,ZED,ZHN,ZHD,ZHNR,ZDEN
      COMPLEX*16  ZE,ZH,ZZZ,ZZX,ZXZ,ZXX
      COMPLEX*16  K11,K12,K22,J,SK11,SK12,SK22,DET
      CHARACTER*8   FNAME
      CHARACTER*12  SNAME
C
      OPEN(1,FILE='DATAIN1',STATUS='OLD')
      PRINT*, 'ENTER OUTPUT DATA FILE NAME  <FNAME>='
      READ*, FNAME
      OPEN(2,FILE=FNAME)
      SNAME=FNAME//'PLT'
      OPEN(3,FILE=SNAME)
C     WRITE(2,*) '   FILE NAME = ',FNAME
C     WRITE(3,*) '   FILE NAME = ',SNAME
C
C     PARAMETERS
      C=3.E8
      J=CMPLX(0.,1.)
      PI=4.*ATAN(1.)
      E0=1.E-9/(36.*PI)
      MU0=4.*PI*1.E-7
C     LIMIT=1.E-2
      LIMIT=1.E-5
      COMPARE=1
      COUNT=1
      LLOG=.TRUE.
C
      CALL READF(W1,W2,L1,L2,A,D,T,H,ER)
      PRINT*,'ENTER THE NUMBER OF OUTER SUM LOOP    N = '
      READ*,N
C     N=20
      WRITE(2,*) 'THE NUMBER OF OUTER SUM LOOP     N =',N
      WRITE(3,*) 'THE NUMBER OF OUTER SUM LOOP     N =',N
C
      PRINT*, 'ENTER THE NUMBER OF INNER SUM LOOP   M = '
```

```
      READ*, M
C     M=20, 40, 100, 500, 1000, 2000, 3000, 4000 ETC.
      WRITE(2,*) 'THE NUMBER OF INNER SUM LOOP     M =',M
      WRITE(3,*) 'THE NUMBER OF INNER SUM LOOP     M =',M
C
      RL=0.10D0
      RRL=RL*1.D3
C
      WRITE(2,*) 'RL = ',RRL
      WRITE(3,*) 'RL = ',RRL
C
1     PRINT*,'ENTER INITIAL FREQUENCY (GHZ)  '
      READ*,F
      F=F*1.E9
C
11    PRINT*,'FREQUENCY = ',F
      WRITE(2,*) 'FREQUENCY = ',F
C
      OMEGA=2.*PI*F
C
      K11=CMPLX(0.,0.)
      K12=CMPLX(0.,0.)
      K22=CMPLX(0.,0.)
C
      DO 20 I=1,N
C        KN=I*PI/A
         KN=(I-.5)*PI/A
C
         JZIN1=COS(KN*W1)-2.*SIN(KN*W1)/(KN*W1)
     +         +2.*(1-COS(KN*W1))/(KN*W1)**2
         JZIN2=COS(KN*W2)-2.*SIN(KN*W2)/(KN*W2)+2.*(1-COS(KN*W2))
     +          /(KN*W2)**2
         JZKN1=2.*SIN(KN*W1)/(KN*W1)+3.*JZIN1/(KN*W1)**2
         JZKN2=2.*SIN(KN*W2)/(KN*W2)+3.*JZIN2/(KN*W2)**2
         JXKN1=-2.*PI*SIN(KN*W1)/(PI**2-(KN*W1)**2)
         JXKN2=-2.*PI*SIN(KN*W2)/(PI**2-(KN*W2)**2)
C
         SK11=CMPLX(0.,0.)
         SK12=CMPLX(0.,0.)
         SK22=CMPLX(0.,0.)
C
         DO 40 IM=1,M
            BETA=(REAL(IM)-.5)*PI/RL
C           BETA=REAL(IM)*PI/RL
C
            GAM1S=KN**2+BETA**2-E0*MU0*OMEGA**2
C
            CALL GAMCT(GAMA1,GAM1S,CT1,D)
C
            CALL GAMCT(GAMA3,GAM1S,CT3,H)
C
            GAM2S=KN**2+BETA**2-E0*MU0*ER*OMEGA**2
C
            CALL GAMCT(GAMA2,GAM2S,CT2,T)
C
            ZEN=GAMA2*CT1/ER + GAMA1*CT2
            ZENR=-J/(OMEGA*E0)
            ZED=CT1*CT2+CT1*CT3*GAMA2/(GAMA3*ER)
     +           +CT2*CT3 + ER*GAMA1/GAMA2
            ZE=ZENR*ZEN/ZED
```

```
C
            ZHN=GAMA1*CT1 +GAMA2*CT2
            ZHNR=J*OMEGA*MU0
            ZHD=GAMA1*CT1*GAMA2*CT2 + GAMA1*CT1*GAMA3*CT3
     +           + GAMA2*CT2*GAMA3*CT3 + GAMA2**2
            ZH=ZHNR*ZHN/ZHD
C
            ZDEN=KN**2 + BETA**2
            ZZZ=-(ZE*BETA**2 + ZH*KN**2)/ZDEN
            ZZX=-KN*BETA*(ZE-ZH)/ZDEN
            ZXZ=ZZX
            ZXX=-(ZE*KN**2 + ZH*BETA**2)/ZDEN
C
            JZBE1=4.*PI*COS(BETA*L1)/(PI**2-(2.*BETA*L1)**2)
            JZBE2=4.*PI*COS(BETA*L2)/(PI**2-(2.*BETA*L2)**2)

            JZ1=JZKN1*JZBE1+JZKN2*JZBE2
            JZ1=JZ1*0.5D0
            JXBE1=COS(BETA*L1/2.)/(BETA*L1/2.)
     +        - SIN(BETA*L1/2.)/(BETA*L1/2.)**2
            JXBE2=COS(BETA*L2/2.)/(BETA*L2/2.)
     +        - SIN(BETA*L2/2.)/(BETA*L2/2.)**2

            JX1=JXKN1*JXBE1+JXKN2*JXBE2
C
            SK11=SK11+JZ1*ZZZ*JZ1
            SK12=SK12+JZ1*ZZX*JX1
            SK22=SK22+JX1*ZXX*JX1
40        CONTINUE
C
C     WRITE(2,*) JZ1,JX1

            K11=K11+SK11
            K12=K12+SK12
            K22=K22+SK22
20      CONTINUE
C
        PRINT*, 'CHECK K11 = ',K11
        WRITE(2,*) 'CHECK K11 = ',K11
        PRINT*, 'CHECK K12 = ',K12
        WRITE(2,*) 'CHECK K12 = ',K12
        PRINT*, 'CHECK K22 = ',K22
        WRITE(2,*) 'CHECK K22 = ',K22
C
C
        DET=K11*K22-K12*K12
        PRINT*, 'DET = ',DET
        WRITE(2,*) 'DETERMINENT = ',DET
C
C
        CALL FDSORT(F,DET,COUNT)
        COUNT=COUNT+1
C
C
        IF (LLOG) THEN
           PRINT*, 'MAKE SURE OPPOSITE SIGNS BETWEEN 1ST & 2ND DETS'
           PRINT*, 'IF SAME SIGNS THEN ENTER 9 , OR ENTER 0'
```

```
C
         READ*, IJK
         IF (IJK.EQ.9) THEN
            OLDF=F
            GOTO 1
         ENDIF
         LLOG=.FALSE.
      ENDIF
C
C
      CMP=REAL(DET)
      LIMF=ABS(F-OLDF)
C
      PRINT*, 'CHECK LIMIT FREQ ',LIMF
      WRITE(2,*) 'CHECK LIMIT FREQ = ',LIMF
C
C     IF (ABS(CMP).GT.LIMIT.AND.LIMF.GT.1.E3)  THEN
      IF (ABS(CMP).GT.LIMIT.AND.LIMF.GT.1.E-1)  THEN
        CALL SLVAL(CMP,OLDF,F,NEWF,COMPARE)
         OLDF=F
         F=NEWF
         GOTO 11
      ENDIF
C
      PRINT*, 'LAST FREQUENCY = ',F
      WRITE(2,*) 'LAST FREQUENCY = ',F
C
      CALL FDSORT(F,DET,100)

      STOP
      END


C**********************************************************************
       SUBROUTINE READF(W1,W2,L1,L2,A,D,T,H,ER)
       REAL*8   W1,W2,L1,L2,A,D,T,H,ER
       INTEGER DDDD
       PRINT*,'DATA INPUT : KEYBORD(1),FILE(0)'
       READ*,DDDD
9      IF(DDDD.EQ.0) THEN
           READ(1,*) W1,W2,L1,L2,A,D,T,H,ER
       ELSEIF(DDDD.EQ.1) THEN
           PRINT*,'ENTER THE W1  &  W2'
           READ*,W1,W2
           PRINT*,'ENTER L1  &  L2'
           READ*,L1,L2
           PRINT*,'ENTER A'
           READ*,A
           PRINT*,'ENTER D, T,  &  H'
           READ*,D,T,H
           PRINT*,'ENTER  ER'
           READ*,ER
        ELSE
          PRINT*,'SELECT  1  OR  0 '
          READ*, DDDD
          GO TO  9
        ENDIF

        PRINT 32, W1,W2,L1,L2,A,D,T,H,ER
        WRITE(2,32) W1,W2,L1,L2,A,D,T,H,ER
        WRITE(3,32) W1,W2,L1,L2,A,D,T,H,ER
```

```
        W1 = W1*1.E-3/2.
        W2 = W2*1.E-3/2.
        L1 = L1*1.E-3
        L2 = L2*1.E-3
        A = A*1.E-3/2.
        D = D*1.E-3
        T = T*1.E-3
        H = H*1.E-3
32    FORMAT(T3,'UNIT:MILIMETER'
     +    ,/,T3,'W1 = ',F9.5,5X,'W2 = ',F9.5
     +    ,/,T3,'L1 = ',F9.5,5X,'L2 = ',F9.5
     +    ,/,T3,'A = ',F9.5
     +    ,/,T3,'D = ',F9.5,5X,'T = ',F9.5,5X,'H = ',F9.5
     +    ,/,T3,'ER = ',F9.5,/)
      RETURN
      END
C*****************************************************************
      SUBROUTINE GAMCT(GAMA,GAMS,CT,LENGTH)
      COMPLEX*16  GAMA,CT
      REAL*8   GAMS,LENGTH,GAMR,CTR

      GAMR =DSQRT(DABS(GAMS))
      IF(GAMS.LT.0.D0) THEN

         GAMA = CMPLX(0.D0,GAMR)
         CTR = -1./TAN(GAMR*LENGTH)
         CT = CMPLX(0.D0,CTR)
       ELSE
         GAMA = CMPLX(GAMR,0.D0)
         CTR = 1./TANH(GAMR*LENGTH)
         CT = CMPLX(CTR,0.D0)

       ENDIF
       RETURN
       END
C*****************************************************************
      SUBROUTINE SLVAL(FUN,OXV,XV,NEWXV,SN)
      INTEGER    SN
      REAL*8     FUN,OXV,XV,NEWXV,POSXV,NEGXV
      IF(SN.EQ.1) THEN
       IF(FUN.GT.0.) THEN
            POSXV = XV
            NEGXV = OXV
         ELSE
            NEGXV = XV
            POSXV = OXV
        ENDIF
        NEWXV = (POSXV + NEGXV)/2.
        SN = SN +2
      ELSE
        IF(FUN.GT.0.) THEN
          POSXV = XV
        ELSE
          NEGXV = XV
        ENDIF
        NEWXV = (POSXV +NEGXV)/2.
      ENDIF
      RETURN
      END
```

```
C*************************************************************************
      SUBROUTINE  FDSORT(FQY,SDET,ICOUNT)
      INTEGER ICOUNT,IC
      REAL*8    FREQY(100),FQY,RTEMP,MAGDET,TFQY
      COMPLEX*16  DETMT(100),SDET,CTEMP,TSDET
      TFQY = FQY
      TSDET = SDET
     IF(ICOUNT.EQ.1) THEN
       FREQY(1) = TFQY
       DETMT(1) = TSDET
     ELSEIF(ICOUNT.NE.100) THEN
       DO 10 I=1,ICOUNT-1

         RTEMP = FREQY(I)
         CTEMP = DETMT(I)
         IF (RTEMP.GT.TFQY) THEN
             FREQY(I) = TFQY
             TFQY = RTEMP
             DETMT(I) = TSDET
             TSDET = CTEMP
         ENDIF
10     CONTINUE
       FREQY(ICOUNT) = TFQY
       DETMT(ICOUNT) = TSDET
       IC = ICOUNT
     ELSEIF(ICOUNT.EQ.100) THEN
       WRITE(3,110)
       WRITE(3,120)
110    FORMAT(//,T8,'FREQUENCY ',T23,'MAG OF DET ',T43,'DETERMINENT')
120    FORMAT(1X,T40,'RE.',T56,'IM.')
       DO 20 J  =1,IC
         MAGDET =DSQRT(REAL(DETMT(J))**2+DIMAG(DETMT(J))**2)
         WRITE(3,210) FREQY(J),MAGDET,DETMT(J)
210      FORMAT(T5,F15.2,T20,F15.3,T38,2(E15.8))
20     CONTINUE
     ENDIF
     RETURN
     END
```

B. PROPAGATION CONSTANT β

```
FILE: BETA     FOR      A1

      INTEGER  MMAX,NMAX
      REAL*8   W,A,D,T,H,PI,ER,FG,OMG,E0,KN
      REAL*8   G1S2,B0,B00,DBTA,FLAG,AA2,CC,WW
      REAL*8   G1,CT01,CT03,GT1,GT3,G2S2,G2,CT02,KE1,KH1,JZ1
      REAL*8   B,OUT,EREFF,FC,BIN,Q,R
      DIMENSION  B(60),OUT(30)
      COMPLEX*16  GM1,GM3,CT1,CT3,GM2,CT2,DENE,ZE,KE,DENH,ZH,KH
      COMPLEX  TRMN,SUMUP,JZ11
C
      OPEN(2,FILE='BETAVAL',STATUS='OLD')
C
      PI=4.D0*ATAN(1.D0)
      FLAG=0
C
      MMAX=30
      NMAX=30
C
      PRINT*,'ENTER  FREQ.,GHZ.'
      READ*, FG
C
      PRINT*,'ENTER  SHLD.  WDTH(MM)'
      READ*, AA2
      A=AA2/2000
      PRINT*,'ENTER  SHLD.  HT.(MM)'
      READ*,CC
      CC=CC/1.D3
      PRINT*,'ENTER LOWER AIRGAP,(MM)'
      READ*,D
      D=D/1.D3
      PRINT*,'ENTER SUBSTRATE THICKNESS(MM)'
      READ*,T
      T=T/1.D3
      H=CC-(D+T)
      PRINT*,'ENTER THE SUBSTRATE DIELEC. CONST. '
      READ*,ER
      PRINT*,'ENTER THE LINEWIDTH(MM)'
      READ*,WW
      W=WW/2.D3

      Q=0.2077+1.2177*T/CC-0.08364*A*2./CC
      PRINT*,'Q=',Q
      R=0.03451-0.1031*T/CC+0.01742*A*2./CC
      PRINT*,'R=',R
      TT=Q-R*LOG(W*2./CC)
      SS=LOG(1./SQRT(ER))

      EREFF=1./(1+TT*SS)

      EREFF=EREFF**2
      PRINT*, 'EREFF = ',EREFF


      OMG=FG*PI*2E9
```

```
      E0=8.84D-12
C     B0=(OMG/3D8)*SQRT((ER+1)/2)
      B0=(OMG/3D8)*SQRT(EREFF)
      B00=0.20D0
      DBTA=0.10D0
      GO TO 4
  5   B0=BIN
      B00=0.85D0
      DBTA=0.007D0
  4   DO  2  M=1,MMAX
      SUMUP=0
      B(M)=B0*(B00+M*DBTA)
      DO  1  N=1,NMAX
      KN=(N-0.5D0)*PI/A
      G1S2=KN**2+B(M)**2-OMG**2/9D16
      G1=SQRT(ABS(G1S2))
      IF(G1S2.LT.0) THEN
         GM1=CMPLX(0.D0,G1)
         GM3=GM1
         CT01=-1.D0/TAN(G1*H)
         CT03=-1.D0/TAN(G1*D)
         CT1=CMPLX(0.D0,CT01)
         CT3=CMPLX(0.D0,CT03)
      ELSE
         GM1=CMPLX(G1,0.D0)
         GT1=1.D0/TANH(G1*H)
         GM3=GM1
         GT3=1.D0/TANH(G1*D)
         CT1=CMPLX(GT1,0.D0)
         CT3=CMPLX(GT3,0.D0)
      ENDIF
C
      G2S2=KN**2+B(M)**2-ER*OMG**2/9.D16
      G2=SQRT(ABS(G2S2))
      IF (G2S2.LT.0) THEN
         GM2=CMPLX(0.D0,G2)
         CT02=-1.D0/TAN(G2*T)
         CT2=CMPLX(0.D0,CT02)
      ELSE
         GM2=CMPLX(G2,0.D0)
         GT2=1.D0/TANH(G2*T)
         CT2=CMPLX(GT2,0.)
      ENDIF
C
      DENE=CT2*CT3+CT1*CT3*(GM2/GM1)/ER+CT1*CT2+(GM3/GM2)*ER
      ZE=(GM2*CT3/ER+GM3*CT2)/DENE
      KE1=-1.D0/(OMG*E0)
      KE=CMPLX(0.D0,KE1)
      ZE=KE*ZE
      DENH=GM1*CT1*GM2*CT2+GM1*CT1*GM3*CT3+GM2*CT2*GM3*CT3+GM2**2
      ZH=(GM2*CT2+GM3*CT3)/DENH
      KH1=OMG*PI*4D-7
      KH=CMPLX(0.D0,KH1)
      ZH=ZH*KH
      JZ1=COS(KN*W)-2.D0*SIN(KN*W)/(KN*W)+2.D0*(1.-COS(KN*W))/(KN*W)**2
      JZ1=2.D0*SIN(KN*W)/(KN*W)+3.D0/((KN*W)**2)*JZ1
      JZ11=CMPLX(JZ1,0.D0)
      TRMN=-(B(M)**2*ZE+KN**2*ZH)/(B(M)**2+KN**2)*JZ11**2
      SUMUP=TRMN+SUMUP
  1   CONTINUE
C
```

```
      OUT(M)=CABS(SUMUP)
    2 CONTINUE
C
      DO  3  M=2,(MMAX-1)
      IF ((OUT(M).LT.OUT(M-1)).AND.(OUT(M).LT.OUT(M+1))) THEN
         BIN=B(M)
      ELSE
      ENDIF
    3 CONTINUE
C
      IF (FLAG.EQ.0) THEN
         FLAG=1.D0
         GO TO 5
      ELSE
         PRINT*,'SUSP. STRIPLINE BETA = ',BIN
         WRITE(2,*)  'SUSP. STRIPLINE BETA = ',BIN
      ENDIF
      STOP
      END
```

C. EQUIVALENT CIRCUIT CAPACITANCE & INDUCTANCE

```
FILE: EQICIR   FOR      A1

      INTEGER  I
      REAL*8   BETA1,BETA2,Z01,Z02
      REAL*8   PI,F,OMEGA,W1,W2
      COMPLEX*16   A,B,C,J,Z3,Z4,NUMZ3,DENZ3,NUMZ4,DENZ4
      COMPLEX*16   CAPAC,INDUC,WC,WL
      DIMENSION  A(3),B(3),C(3)
      CHARACTER*8   FNAME
      PRINT*, 'ENTER OUTPUT DATA FILE NAME'
      READ*,FNAME
      OPEN(2,FILE=FNAME)
      J=CMPLX(0.D0,1.D0)
      PI=4.D0*ATAN(1.D0)
      PRINT*,'ENTER RES. FREQUENCY (GHZ)'
      READ*,F
      WRITE(2,*) 'RESONANT  FREQUENCY(GHZ) =',F
      F=F*1.E9
      OMEGA=2.D0*PI*F
C
      PRINT*,'ENTER W1 & W2'
      READ*,W1,W2
      WRITE(2,130) W1,W2
 130  FORMAT(T3,'W1 = ',F3.1,'MM',5X,'W2 = ',F6.4,'MM')
      PRINT*, 'ENTER Z01 & Z02'
      READ*, Z01,Z02
      PRINT*,'Z01 = ',Z01
      PRINT*,'Z02 = ',Z02
      WRITE(2,100)  Z01,Z02
 100  FORMAT(T3,'Z01 = ',F8.4,5X,'Z02 = ',F8.4)
      PRINT*, 'ENTER BETA1 & BETA2'
      READ*, BETA1,BETA2
      PRINT*, 'BETA1 = ',BETA1
      PRINT*, 'BETA2 = ',BETA2
      WRITE(2,110) BETA1,BETA2
 110  FORMAT(T3,'BETA1 = ',F8.4,5X,'BETA2 = ',F8.4)
      DO 10  I=1,3,1
      CALL  Z1Z2ABC(BETA1,BETA2,Z01,Z02,J,I,A,B,C)

 10   CONTINUE
      NUMZ3=(C(1)-C(3))*(B(1)-B(2))-(C(1)-C(2))*(B(1)-B(3))
      DENZ3=(A(1)-A(3))*(B(1)-B(2))-(A(1)-A(2))*(B(1)-B(3))
C     NUMZ3=(C(1)-C(2))*(B(2)-B(3))-(C(2)-C(3))*(B(1)-B(2))
C     DENZ3=(A(1)-A(2))*(B(2)-B(3))-(A(2)-A(3))*(B(1)-B(2))
      Z3=NUMZ3/DENZ3
      NUMZ4=(C(1)-C(2))-Z3*(A(1)-A(2))
      DENZ4=B(1)-B(2)
      Z4=NUMZ4/DENZ4
      PRINT*,'NUMZ3 =',NUMZ3,'DENZ3 =',DENZ3
      PRINT*,'NUMZ4 =',NUMZ4,'DENZ4 =',DENZ4
      WRITE(2,*) 'NUMZ3 =',NUMZ3,'DENZ3 =',DENZ3
      WRITE(2,*) 'NUMZ4 =',NUMZ4,'DENZ4 =',DENZ4
      PRINT*,'Z3 = ',Z3
      PRINT*,'Z4 = ',Z4
```

```
      WRITE(2,*) 'Z3 = ',Z3
      WRITE(2,*) 'Z4 = ',Z4
      CAPAC=1./(Z3*J*OMEGA)
      INDUC=Z4/(J*OMEGA)
      PRINT*, 'CAPAC.= ',CAPAC
      PRINT*, 'INDUC.= ',INDUC
      WRITE(2,*) 'CAPAC. = ',CAPAC
      WRITE(2,*) 'INDUC. = ',INDUC
      WC=1.D0/(OMEGA*CAPAC)
      WL=OMEGA*INDUC
      PRINT*, '1/WC = ',WC
      PRINT*, 'WL = ',WL
      WRITE(2,*) '1/WC = ',WC
      WRITE(2,*) 'WL = ',WL
      STOP
      END


      SUBROUTINE  Z1Z2ABC(BETA1,BETA2,Z01,Z02,J,I,A,B,C)
      INTEGER  I
      REAL*8 BETA1,BETA2,Z01,Z02,L1,L2
      COMPLEX*16  A,B,C,J,Z1,Z2
      DIMENSION  A(3),B(3),C(3)


      PRINT*, 'ENTER L1 & L2 (MM)'
      READ*, L1,L2
      PRINT*, 'L1(MM) = ',L1
      PRINT*, 'L2(MM) = ',L2
      WRITE(2,120)  L1,L2
  120 FORMAT(T3,'L1(MM) = ',F8.4,5X,'L2(MM) = ',F8.4)
      L1=L1/1.D3
      L2=L2/1.D3
      Z1=J*Z01/TAN(BETA1*L1)
      Z2=-J*Z02/TAN(BETA2*L2)
      PRINT*,'Z1 = ',Z1
      PRINT*,'Z2 = ',Z2
      WRITE(2,*)'Z1 = ',Z1
      WRITE(2,*) 'Z2 = ',Z2
      A(I)=CONJG(Z1)-Z2
      B(I)=CONJG(Z1)
      C(I)=-CONJG(Z1)* Z2
      PRINT*,'A(',I,'          ) = ',A(I)
      PRINT*,'B(',I,'          ) = ',B(I)
      PRINT*,'C(',I,'          ) = ',C(I)
      WRITE(2,*) 'A(',I,'          ) = ',A(I)
      WRITE(2,*) 'B(',I,'          ) = ',B(I)
      WRITE(2,*) 'C(',I,'          ) = ',C(I)
      RETURN
      END
```

LIST OF REFERENCES

1. Tatsuo Itoh, "Analysis of Microstrip Resonators", IEEE Trans. Microwave Theory and Technique, vol. MTT-22, pp. 946-952 (1974).

2. Tatsuo Itoh, *Numerical Techniques for Microwave Passive Structures,* John Wiley & Sons., Chapter 5, 1989.

3. Tatsuo Itoh and R. Mittra, "A Technique for Computing Dispersion Characteristics of Shielded Microstrip Lines", IEEE Trans. Microwave Theory and Tech., vol. MTT-21, pp.496-499, July 1973.

4. Y. Shu, Y. Qi, Y. Wang, "Analysis Equations for Suspended Substrate Microstrip line and Broadside-coupled Stripline", IEEE Microwave Theory and Tech. Symposium Digest, pp. 693-696 (1987).

5. Fred E. Gardiol, "Careful MIC Design Prevents Waveguide Modes", Microwaves, pp. 188-190, May 1977.

6. Harry A. Atwater, *Introduction to Microwave Theory,* Robert E. Krieger Publishing Co., 1981.

7. C. Gupta, and A. Gopinath, "Equivalent Circuit Capacitance of Microstrip Step Change in Width", IEEE Trans. on Microwave Theory and Tech., vol. MTT-25, pp. 819-822 (1977).

8. Reinmut K. Hoffmann, *Handbook of Microwave Integrated Circuits*, Artech House, Chapter 10, 1990.

9. Man Su Choi, *Computer Aided Design Models for Millimeter-wave Suspended Substrate Microstrip Line,* M.S.E.E. Thesis, Naval Postgraduate School, CA., March 1990.

10. Jae Soon Jeong, *An Evaluation of Coplanar Line for Application in Microwave Integrated Circuitry,* M.S.E.E. Thesis, Naval Postgraduate School, CA., December 1988.

INITIAL DISTRIBUTION LIST

		No. Copies
1.	Defense Technical Information Center Cameron Station Alexandria, VA 22304-6154	2
2.	Library, Code 52 Naval Postgraduate School Monterey, CA. 93943-5002	2
3.	Professor Harry A. Atwater, Code /An Department of Electrical and Computer Engineering Naval Postgraduate School Monterey, CA. 93943-5000	2
4.	Professor Rama Janaswamy,Code EC/Js Department of Electrical and Computer Engineering Naval Postgraduate School Monterey, CA. 93943-5000	1
5.	Library of Korea Military Academy P.O.Box 77 Kongneung-dong Dobong-gu Seoul, Republic of Korea	1
6.	Cdr Uwe Becker c/o Federal Republic of Germany Military Representative, S1-pers.o.V.I.A 4000 Brandywine., N.W. Washington, D.C. 20016-1887	1
7.	Ltc Carlos Augusto Teixeira Rua Farani 60-A.P. 904 Ria de Janeiro-RJ Brasil	1

8. Cdr Chen-Kuo Yu — 1
4F-2, 282, Tung-Men Rd.
Ku-Shan, Kaohsiung,
Taiwan 80401
Republic of China

9. Cdr Harry Thornberry — 1
Clemente X 335
San Isidro
Lima
Peru

10. Ltcdr Sudjiwo — 1
Kompleks TNI-Al No. 17B
Radio Dalam
Kebayoran Baru
Jakarta-Selatan 12140
Indonesia

11. Maj Geraldo Batista — 1
Rua Alferes Esteves, 313
35660 Para de Minas-MG
Brasil

12. Ltcdr Kamran Kahn — 1
1-C-4/11
Nazimabad
Karachi
Pakistan

13. Ltcdr Ramesh Kumar — 1
B-5-22
Nausanrakshan Society
NearLiberty Gaqoen
Malao West
Bombay
India

14. Lt Juan Jose Sanchez
Calle 3, No. 46, Qta Lidice
Urb. Chucho Briceno
(1, EtApa), Cp. 3002
Venezuela — 1

15. Lt Mauricio Gaviria
Calle 71 #4-47
Bogota, DE
Colombia, S.A. — 1

16. Jin, Won Tae
377-1 Jangseungpo-si Kyungnam-do
Seoul, Republic of Korea — 5